

Spontaneous synchronization and nonequilibrium statistical mechanics of coupled phase oscillators

Stefano Gherardini^a, Shamik Gupta^b and Stefano Ruffo^{c*}

^aDepartment of Physics, University of Florence, via S. Marta 3, I-50139 Florence, INFN and LENS, via G. Sansone 1, I-50019 Sesto Fiorentino, Italy

^bDepartment of Physics, Ramakrishna Mission Vivekananda University, Belur Math, Howrah 711202, India

^cSISSA, via Bonomea 265, CNISM and INFN, I-34136 Trieste, Italy

ARTICLE HISTORY

Compiled May 18, 2018

ABSTRACT

Spontaneous synchronization is a remarkable collective effect observed in nature, whereby a population of oscillating units, which have diverse natural frequencies and are in weak interaction with one another, evolves to spontaneously exhibit collective oscillations at a common frequency. The Kuramoto model provides the basic analytical framework to study spontaneous synchronization. The model comprises limit-cycle oscillators with distributed natural frequencies interacting through a mean-field coupling. Although more than forty years have passed since its introduction, the model continues to occupy the centre-stage of research in the field of non-linear dynamics, and is also widely applied to model diverse physical situations. In this brief review, starting with a derivation of the Kuramoto model and the synchronization phenomenon it exhibits, we summarize recent results on the study of a generalized Kuramoto model that includes inertial effects and stochastic noise. We describe the dynamics of the generalized model from a different yet a rather useful perspective, namely, that of long-range interacting systems driven out of equilibrium by quenched disordered external torques. A system is said to be long-range interacting if the inter-particle potential decays slowly as a function of distance. Using tools of statistical physics, we highlight the equilibrium and nonequilibrium aspects of the dynamics of the generalized Kuramoto model, and uncover a rather rich and complex phase diagram that it exhibits, which underlines the basic theme of intriguing emergent phenomena that are exhibited by many-body complex systems.

KEYWORDS

synchronization, statistical physics, nonequilibrium stationary state, phase transition

Contents

1	Introduction: Spontaneous synchronization	2
2	Theoretical modelling: From limit cycles to the Kuramoto model	3
3	Synchronization in the Kuramoto model and the associated phase transition	9
3.1	Analysis in the thermodynamic limit	11
3.2	Noisy Kuramoto model	15
4	Generalized Kuramoto model with inertia and noise	16
4.1	The model as a long-range interacting system	17

*Corresponding author; e-mail: ruffo@sissa.it

4.2	Dynamics in a reduced parameter space	18
4.3	Nonequilibrium first-order synchronization phase transition	19
4.4	Analysis in the continuum limit: The Kramers equation	22
4.5	$\sigma = 0$: Stationary solutions and the associated phase transition	23
4.6	$\sigma \neq 0$: Incoherent stationary state and its linear stability	24
4.7	$\sigma \neq 0$: Synchronized stationary state	25

5 Conclusions **28**

1. Introduction: Spontaneous synchronization

Spontaneous synchronization is a general phenomenon in which a population of coupled oscillators (usually of different frequencies) self-organizes to operate in unison [1, 2, 3, 4]. The phenomenon is observed in physical and biological systems over a wide range of spatial and temporal scales, e.g., metabolic synchrony in yeast cell suspensions [5], flashing fireflies [6], Josephson junction arrays [7], laser arrays [8], and others. Besides the synchronous firings of cardiac cells that keep the heart beating and life going on [9], synchrony is desired in many man-made systems, e.g., in parallel computing, whereby computer processors must coordinate to finish a task on time, and in electrical power-grids, in which generators must run in synchrony to be locked to the grid frequency [10, 11]. Synchrony could also be hazardous, e.g., in neurons, leading to impaired brain function in Parkinson’s disease and epilepsy. Collective synchrony in oscillator networks has attracted immensely the attention of physicists and applied mathematicians, and finds applications in many fields, from quantum electronics to electrochemistry, from bridge engineering to social science.

This paper provides a basic overview of the field of synchronization from the point of view of a paradigmatic model for analytical studies, the Kuramoto model. The model comprises limit-cycle oscillators with distributed natural frequencies interacting through a mean-field coupling [12]. Since its introduction about forty years ago, the model has been widely employed in the arena of non-linear dynamical system studies to study the phenomenon of spontaneous synchronization, and continues to inspire new expedition to the kingdom of many-body complex systems. This brief review starts with a summary of useful dynamical features of synchronizing systems, followed by a discussion of how they may lead to a derivation of the Kuramoto model. A detailed discussion follows of the synchronization phenomenon exhibited by the model and also its extended version in which the dynamics proceeds in presence of stochastic noise. We devote the rest of the paper to a study of a generalized Kuramoto model that includes inertial effects and stochastic noise, thereby elevating the first-order dynamics of the Kuramoto model to one that is second order in time. We describe the dynamics of the generalized model from a different yet a rather useful perspective, namely, that of long-range interacting systems driven out of equilibrium by quenched disordered external torques. This connection helps to study the model from the point of view of statistical physics, besides offering to form a bridge with a related but until now a largely unconnected field of long-range interacting systems. In fact, we show that in proper limits, the generalized model quite remarkably reduces to the Kuramoto model as well as to a prototypical system with long-range interactions, the Hamiltonian mean-field model [13]. Using tools of statistical physics, we highlight the equilibrium and nonequilibrium aspects of the dynamics of the generalized Kuramoto model. Further, we uncover a rather rich and complex phase diagram that the model exhibits, demarcating regions of parameter space that allow for the emergence of spontaneous synchronization.

The paper is organized as follows. In Section 2, we discuss some general features of synchronizing systems and the derivation of the Kuramoto model. In Section 3, we discuss the analysis of the model in the thermodynamic limit, thereby obtaining the conditions on the parameters of its dynamics that allow for the observation of collective synchrony and an associated phase transition

in the stationary state. Here, we also discuss the case of the noisy Kuramoto model. Section 4 contains detailed discussions on the generalized Kuramoto model. The paper ends with conclusions in Section 5.

2. Theoretical modelling: From limit cycles to the Kuramoto model

It is clear from the aforementioned examples of synchronizing systems that their constituent units are capable of exhibiting oscillations that have a characteristic waveform, amplitude and frequency of oscillation. The latter features depend of course on the physical manifestation of the unit: the heart does not beat the same way as a firefly flashes on and off. Moreover, these characteristic oscillations are such that any (slight) perturbations away from them would soon return the motion to the oscillatory behavior. The dynamics of the individual units should therefore be such as to allow for oscillations that have a characteristic waveform independent of any typical initial condition of the dynamics. Think of the pendulum of a metronome: irrespective of the initial deflection of its pendulum (provided it is not so drastic that you break the metronome !), the latter would soon tick and tock back and forth at a given period, exhibiting oscillations that have both a characteristic amplitude and a characteristic frequency.

Now, one may wonder: How should the underlying dynamics be such as to generate oscillations with a characteristic waveform? On the basis of physical intuition, one may anticipate (correctly) that the dynamics ought to have suitable dissipation and energy-pumping mechanisms so that oscillations that tend to become too large are effectively damped down by dissipation, just as the ones that tend to become too small are suitably pumped up by a supply of energy. As a result, oscillations of a characteristic form, for which pumping and damping effects balance each other, are only sustained. The presence of damping at once precludes the possibility for the underlying dynamics to be conservative, i.e., a dynamics given by the Hamilton equations of motion corresponding to a suitable system Hamiltonian. Consequently, the stationary state that the dynamics relaxes to at long times would not be an equilibrium one, but would be a generic nonequilibrium stationary state (NESS) [14]. The reader may recall that the basic tenet of classical equilibrium statistical mechanics is a dynamics modelled by the Hamilton equations of motion derived from the Hamiltonian of the system under consideration.

Let us illustrate with an example how a dynamics that incorporates dissipation and energy-pumping mechanisms leads to oscillations of a characteristic form independent of initial conditions. Consider a single dynamical degree of freedom $x(t)$ describing the displacement from equilibrium of a damped, driven harmonic oscillator, whose time evolution is given by the so-called Van der Pol equation:

$$\frac{d^2x}{dt^2} - (\gamma - x^2) \frac{dx}{dt} + \omega^2 x = 0. \quad (1)$$

Here, the parameter γ is a real positive constant, while the parameter ω is real. In the dynamics (1), note that the second term changes sign depending on whether x has a magnitude smaller or larger than a characteristic value equal to $\sqrt{\gamma}$. As a result, the dynamics pumps up small displacements (i.e., with $|x| < \sqrt{\gamma}$) and damps down the large ones (i.e., with $|x| > \sqrt{\gamma}$). Hence, independently of initial conditions, the dynamics for given values of γ and ω approaches asymptotically in time a state that supports oscillations with a characteristic amplitude and a characteristic frequency. In other words, the solution $x(t)$ of the dynamics (1) becomes in the long-time limit a periodic motion with a characteristic waveform, see Fig. 1(a).

The dynamics (1) may be written in terms of a set of two coupled first-order differential equa-

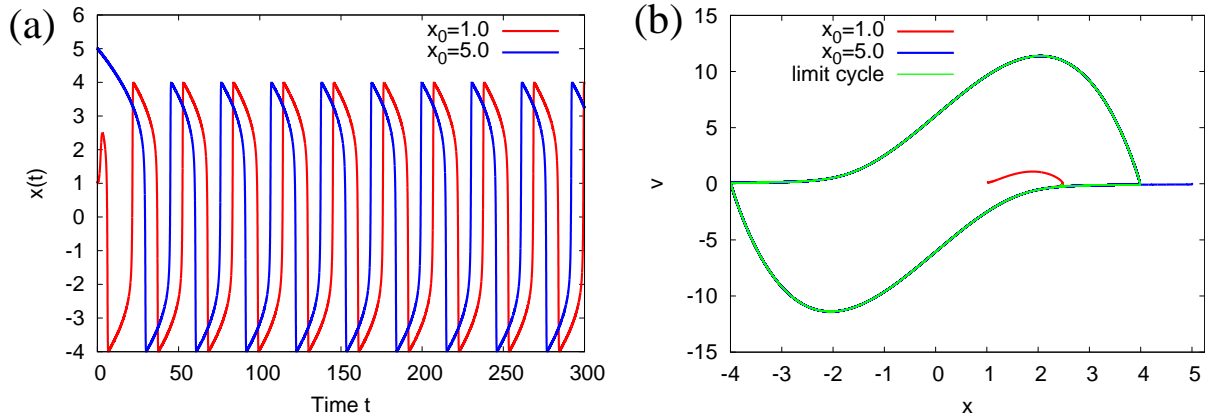


Figure 1. The Van der Pol oscillator dynamics, Eq. (1) (equivalently, Eq. (2)), showing for two different initial values x_0 of the position and a given initial value $v_0 = 0.1$ of the velocity (a) the displacement x as a function of time, and (b) the trajectory traced out in the phase space (x, v) by the initial point (x_0, v_0) . In panel (a), one may observe that independently of initial conditions, the dynamics in a short time settles into oscillations of a characteristic waveform. Correspondingly, one has in panel (b) an eventual relaxation to a motion along a limit cycle; for large times, the motion is virtually indistinguishable from the limit cycle. The data are obtained by numerical integration of Eq. (2) for parameter values $\gamma = 4.0, \omega = 0.5$.

tions, by introducing the velocity variable v as follows:

$$\frac{dx}{dt} = v, \quad \frac{dv}{dt} = (\gamma - x^2)v - \omega^2 x. \quad (2)$$

Then, in the phase space of the system, given by the two-dimensional plane $(x_1, x_2) \equiv (x, v)$, the dynamical trajectory/orbit traced out by an initial point (x_0, v_0) may be seen to approach asymptotically in time a stable periodic orbit that is in one-to-one mapping with the long-time periodic solution discussed above. Oscillations that have a characteristic waveform, amplitude and frequency, and are thus represented by a characteristic periodic orbit in the phase space are said to define the so-called limit-cycle oscillators [15]. We may thus say that any initial condition evolving under the dynamics (1) eventually relaxes to a motion around a limit cycle given by the aforementioned periodic orbit. In particular, an orbit starting close to the limit cycle gets after a very short time extremely close to the cycle and becomes essentially indistinguishable from the latter, although mathematically speaking, it never reaches it due to the uniqueness of solutions of the dynamics. The limit cycle is stable in the sense that any (small) perturbations away from it decay in time, thereby attracting all neighboring orbits towards it under the dynamical evolution. A limit cycle can also be unstable, whereby all neighboring orbits are repelled away from it under dynamical evolution [15]. Figure 2, panels (a) and (b) compare a stable and an unstable limit cycle. The limit cycle for dynamics (1) is shown in Fig. 1(b).

A limit cycle is evidently an *isolated* periodic orbit in the phase space. These cycles can occur only in non-linear dynamical systems. A linear dynamics $dx_\alpha/dt = \sum_{\alpha,\beta} A_{\alpha\beta} x_\beta$ can of course generate periodic orbits, but since with every periodic orbit $\{x_\alpha(t)\}$, one may associate a family of periodic orbits $\{cx_\alpha(t)\}$ with c a parameter, such an orbit would not be isolated, but would be surrounded by an infinite number of periodic orbits obtained by varying c . The issue of which one among the orbits is chosen by the dynamics is set by its initial condition, unlike the independence of the form of a limit cycle with respect to initial conditions. Also, any slight perturbation away from such a closed orbit will unlike a limit cycle not return the motion to the orbit, but will take it to a neighboring closed orbit.

The above comments on the definition and properties of a limit cycle and the nature of the

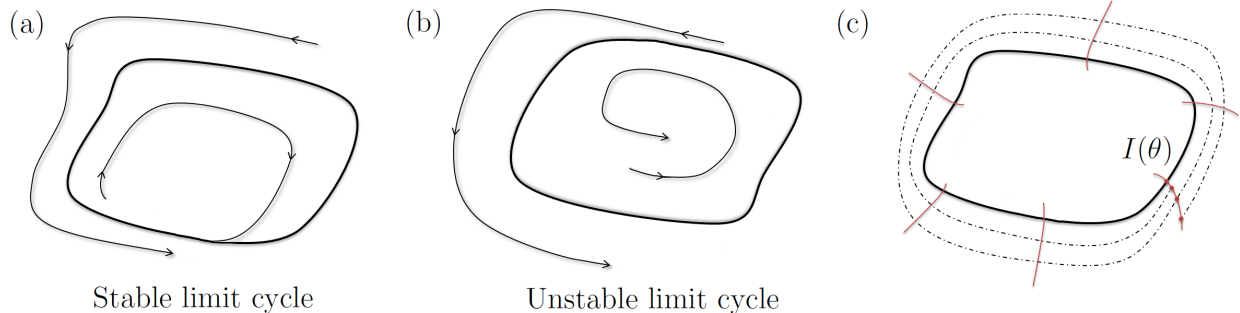


Figure 2. Panels (a) and (b) compare the dynamics around a stable and an unstable limit cycle. While nearby trajectories under dynamical evolution are attracted towards a stable limit cycle, they are instead repelled away from the cycle when it is unstable. In panel (c), we illustrate the construction of isochrones for a stable limit cycle.

dynamics leading to it also apply to a generic autonomous dynamical system comprising many interacting degrees of freedom $\{x_\alpha\}_{1 \leq \alpha \leq n}$; $n \gg 1$, with a dynamics given by [15]

$$\frac{dx_\alpha}{dt} = F_\alpha(x_1, x_2, \dots, x_n). \quad (3)$$

By autonomous is meant that the functions F_α do not depend explicitly on time.

For a given initial condition $\{x_\alpha(0)\}$, a solution $\{x_\alpha(t)\}$ of the dynamics (3) defines an orbit in the n -dimensional phase space of the system. Being an autonomous dynamics implies that if $\{x_\alpha(t)\}$ is a solution, so is $\{x_\alpha(t+t_0)\}$ for any t_0 , i.e., the choice of the origin of time is irrelevant. Such a property holds either when there is no external influence on the system so that its motion depends solely on the interaction between its constituents, or, even when there is an external influence, it does not depend explicitly on time. Limit cycles denote a particular class of solutions $\{x_{\alpha,0}(t)\}$ represented by one-dimensional periodic orbits in the phase space that satisfy $x_{\alpha,0}(t+T) = x_{\alpha,0}(t) \forall \alpha$, where T is the period of the motion. In the following, any mention of oscillator would mean a stable limit-cycle oscillator, unless stated otherwise.

Consider a limit cycle with period T . The length of the orbit traversed in the phase space in time t is given by $s(t) = \int_0^t dt' \sqrt{\sum_{\alpha=1}^n (dx_\alpha/dt')^2}$, where the freedom in choosing the origin of time translates to the one in the choice of the origin from which the orbit length is measured. Note that $s(pT) = ps(T)$, where p is a positive integer, and that the time rate of variation of s is in general not a constant along the limit cycle. One may however transform to a new variable $\theta = \theta(s)$ whose time rate of variation along the limit cycle is a constant called the *natural frequency* $\omega \equiv 2\pi/T$ of the cycle. Using $\theta(s) \equiv (2\pi/T) \int_0^s ds' / \left[\left(\frac{ds}{dt} \right) (s') \right]$, we have indeed $d\theta/dt = (d\theta/ds)(ds/dt) = 2\pi/T = \omega$. Moreover, defining $s_0 \equiv s(T)$, one has $\theta(s_0) = 2\pi$. Thus, at the end of one time period T , the value of θ increases by 2π , corresponding to one complete traversal of the periodic orbit. We thus arrive at an important conclusion that a limit-cycle oscillator is completely characterized by a phase $\theta \in [-\pi, \pi]$ that changes uniformly in time with period T and frequency ω , as

$$\frac{d\theta}{dt} = \omega. \quad (4)$$

In this paper, the word ‘phase’ would be used to also refer to a thermodynamic phase of a macroscopic system, defined as a region in the space of dynamical parameters throughout which all

macroscopic observable properties of the system are essentially the same. To avoid any possible confusion between the two different usages of the word ‘phase,’ we will from now on use the term ‘angle’ to mean oscillator phase, and the term ‘phase’ to exclusively mean a thermodynamic phase.

Since we may associate a unique value of the angle with each point on the limit cycle, we have $\theta = \theta(\{x_{\alpha,0}\})$. From Eq. (4), it follows that θ is a neutrally stable variable: any (small) perturbations to it neither grow nor decay in time. This property is related to the invariance discussed above of solutions of autonomous dynamical systems with respect to time shifts. In contrast to θ , the amplitude of oscillations has a definite stable value on the limit cycle; any (small) perturbations in a direction transverse to the angle decay in time.

An angle description such as above applies even to orbits that are close to the limit cycle. To see this, consider an initial phase-space point sufficiently close to the limit cycle. As the point traverses an orbit in the phase space, we may decide to observe its successive positions only stroboscopically, namely, at times $t = kT$; $k = 1, 2, 3, \dots$. It follows from the attracting property of the limit cycle that the limit of this sequence of points as $k \rightarrow \infty$ is a point on the limit cycle, which according to the discussion above has a particular value of the angle θ . One may then associate this latter value of θ with the sequence of points, which are now said to lie on a $(n - 1)$ -dimensional hypersurface $I(\theta)$ called an isochrone [1]. Figure 2(c) illustrates the construction of isochrones. In this way, we may associate an angle θ to each point of the phase space lying in close neighborhood of the limit cycle, and consequently, Eq. (4) remains valid also in close neighborhood of the limit cycle.

Having explained the angle description in the context of individual limit-cycle oscillators, we now make an observation that will prove to be quite relevant in our later discussion on oscillators interacting weakly with one another. To this end, consider a limit-cycle oscillator subject to a forcing that is *weak*, which could be due to an external agent or is generated due to the interaction of the oscillator with other oscillators. Owing to the neutral stability of the angle of the limit cycle, even a weak forcing can result in it undergoing *large* changes. This may be contrasted with the corresponding effect on the amplitude of oscillations of the limit cycle, which due to the transversal stability of the cycle is only slightly affected by the external forcing. As a result, even in the presence of a forcing, so long as it is weak, one is justified to continue characterizing the dynamics of the oscillator solely in terms of an angle motion along the limit cycle of the isolated system, and to disregard to leading order any perturbation due to the forcing in a direction transversal to the isolated cycle. This so-called phase approximation for weak forcing allows to derive the dynamics of a population of nearly-identical weakly-interacting limit-cycle oscillators [16, 17], as we now do in the following.

Consider a collection of N nearly-identical limit-cycle oscillators occupying the nodes of a network and interacting weakly with one another, with all the oscillators having the same number n of degrees of freedom. Since the oscillators are nearly identical, they will have dynamical properties that are only slightly different from one another, with differences being of $O(\varepsilon)$, where ε is a small parameter. In the following, we use Greek letters to denote the different degrees of freedom and Latin letters to denote the different oscillators. The j -th oscillator, $j = 1, 2, \dots, N$, having degrees of freedom denoted by the set $\{x_{j\alpha}\}_{1 \leq \alpha \leq n}$, may be considered to have the time evolution given by

$$\frac{dx_{j\alpha}}{dt} = F_{j\alpha}(\{x_{j\beta}\}) + \varepsilon \sum_{k=1, k \neq j}^N \sum_{\beta=1}^n G_{j\alpha, k\beta}(\{x_{j\gamma}\}, \{x_{k\gamma}\}), \quad (5)$$

where the functions $F_{j\alpha}(\{x_{j\beta}\})$ describe the dynamics of the isolated oscillators, while the function $G_{j\alpha, k\beta}(\{x_{j\gamma}\}, \{x_{k\gamma}\})$ represents the influence of the k -th oscillator on the j -th one, with the small parameter ε ensuring that the oscillators are interacting only weakly with one another. From Eq. (5), it is evident that $1/\varepsilon$ has the dimension of time. Now, ε being very small, we may expect $1/\varepsilon$ to be longer than any other characteristic timescale in the dynamics. Since the oscillators have dynamical

properties that are only slightly different, of $O(\varepsilon)$, we may write

$$F_{j\alpha}(\{x_{j\beta}\}) = F_\alpha(\{x_{j\beta}\}) + \varepsilon f_{j\alpha}(\{x_{j\beta}\}), \quad (6)$$

expressing the heterogeneity of individual oscillators as small fluctuations, denoted by $\varepsilon f_{j\alpha}(\{x_{j\beta}\})$, about their common dynamical features given by the functions F_α . Equation (5) then yields

$$\frac{dx_{j\alpha}}{dt} = F_\alpha(\{x_{j\beta}\}) + \varepsilon \left[f_{j\alpha}(\{x_{j\beta}\}) + \sum_{k=1, k \neq j}^N \sum_{\beta=1}^n G_{j\alpha, k\beta}(\{x_{j\gamma}\}, \{x_{k\gamma}\}) \right]. \quad (7)$$

Now, let us assume that the common dynamics $dx_\alpha/dt = F_\alpha(\{x_\beta\})$ allows for a stable limit cycle characterized by the angle θ , with the associated dynamical degrees of freedom denoted by the set $\{x_{\alpha,0}\}$. The angle θ evolves in time as $d\theta/dt = \omega$, where ω is the natural frequency of the limit cycle of the common dynamics; we denote the corresponding time period by $T \equiv 2\pi/\omega$.

Consider a phase-space point $\{x_{j\beta}\}$ close to the limit cycle of the common dynamics. As the phase-space point moves in time, it will owing to the smallness of ε continue to lie close to the limit cycle, moving between a family of isochrones $I(\theta_j)$ defined for the limit cycle and characterized by different values of the angle. As a result, one has the functional dependence $\theta_j = \theta_j(\{x_{j\beta}\})$. Using $d\theta_j/dt = \sum_{\alpha=1}^n (\partial\theta_j/\partial x_{j\alpha}) (dx_{j\alpha}/dt)$ and Eq. (7), we get

$$\frac{d\theta_j}{dt} = \sum_{\alpha=1}^n \left(\frac{\partial\theta_j}{\partial x_{j\alpha}} \right) F_\alpha(\{x_{j\beta}\}) + \varepsilon \sum_{\alpha=1}^n \left(\frac{\partial\theta_j}{\partial x_{j\alpha}} \right) \left[f_{j\alpha}(\{x_{j\beta}\}) + \sum_{k=1, k \neq j}^N \sum_{\beta=1}^n G_{j\alpha, k\beta}(\{x_{j\gamma}\}, \{x_{k\gamma}\}) \right]. \quad (8)$$

Comparing the form of the above equation with Eq. (4), we find that the first term on the right hand side (rhs) equals ω , while to leading order in ε , one may replace the phase-space variables in the second term with their values on the limit cycle. We thus obtain the angle dynamics perturbed by the weak interaction among the oscillators as

$$\frac{d\theta_j}{dt} = \omega + \varepsilon \sum_{\alpha=1}^n Z_\alpha(\theta_j) \left[f_{j\alpha}(\theta_j) + \sum_{k=1, k \neq j}^N \sum_{\beta=1}^n G_{j\alpha, k\beta}(\theta_j, \theta_k) \right]; \quad Z_\alpha(\theta_j) \equiv \left(\frac{\partial\theta_j}{\partial x_{j\alpha}} \right) (\{x_{\gamma,0}\}), \quad (9)$$

where we have $f_{j\alpha}(\theta_j) = f(\{x_{\alpha,0}\}(\theta_j))$ and $G_{j\alpha, k\beta}(\theta_j, \theta_k) = G_{j\alpha, k\beta}(\{x_{\alpha,0}\}(\theta_j), \{x_{\beta,0}\}(\theta_k))$. The small- ε approximation made in writing Eq. (9) entails an error of order ε^2 .

Let us introduce the difference between the oscillator angles θ_j and the steadily increasing component ωt corresponding to in-phase (synchronized) oscillations of all the oscillators, as

$$\psi_j(t) \equiv \theta_j(t) - \omega t. \quad (10)$$

A time-independent ψ_j implies that all the oscillators are oscillating in synchrony with frequency ω . In general, however, ψ_j is time dependent. Equations (10) and (9) yield the time evolution of ψ_j as

$$\frac{d\psi_j}{dt} = \varepsilon \sum_{\alpha=1}^n Z_\alpha(\psi_j + \omega t) \left[f_{j\alpha}(\psi_j + \omega t) + \sum_{k=1, k \neq j}^N \sum_{\beta=1}^n G_{j\alpha, k\beta}(\psi_j + \omega t, \psi_k + \omega t) \right], \quad (11)$$

which combined with the smallness of ε implies that ψ_j varies rather slowly with time, unlike the term ωt that varies rapidly with time. In other words, suppose that at some instant, the oscillators

get synchronized with one another. Such a state will be sustained over times of order $1/\varepsilon$ (which as mentioned above is the longest time interval in the system), during which the term ωt would undergo a large number of changes, namely, of order ω/ε . As a result, over the period $T = 2\pi/\omega$, one may consider all the ψ_j 's to be almost time independent, and so can average Eq. (11) over this period by considering the ψ_j 's to be constant. We arrive at

$$\frac{d\psi_j}{dt} = \varepsilon \left[\Delta_j + \sum_{k=1, k \neq j}^N \Gamma_{jk}(\psi_j - \psi_k) \right]; \quad (12)$$

$$\Delta_j \equiv \frac{1}{T} \int_0^T dt' \sum_{\alpha=1}^n Z_\alpha(\psi_j + \omega t') f_{j\alpha}(\psi_j + \omega t'), \quad (13)$$

$$\Gamma_{jk}(\psi_j - \psi_k) \equiv \frac{1}{T} \int_0^T dt' \sum_{\alpha=1}^n \sum_{\beta=1}^n Z_\alpha(\psi_j + \omega t') G_{j\alpha, k\beta}(\psi_j + \omega t', \psi_k + \omega t'). \quad (14)$$

That the integral on the rhs of Eq. (14) gives a function of the angle difference may be inferred by noting that the angles ψ_j and ψ_k are measured with respect to a zero-angle axis that is arbitrary, and hence, one may choose to measure ψ_k with respect to ψ_j . In doing so, the rhs equals

$$(1/T) \int_0^T dt' \sum_{\alpha=1}^n \sum_{\beta=1}^n Z_\alpha(\omega t') G_{j\alpha, k\beta}(\omega t', \psi_k - \psi_j + \omega t'),$$

which evidently establishes the fact that the rhs of Eq. (14) and hence, Γ_{jk} is a function of the angle difference $\psi_j - \psi_k$. Note that both the functions $Z(\psi)$ and $\Gamma_{jk}(\psi)$ are 2π -periodic in their argument.

Using Eqs. (10) and (12), we may revert to the variables θ_j , and obtain the corresponding dynamical evolution as

$$\frac{d\theta_j}{dt} = \omega_j + \varepsilon \sum_{k=1, k \neq j}^N \Gamma_{jk}(\theta_j - \theta_k), \quad (15)$$

where $\omega_j \equiv \omega + \varepsilon \Delta_j$ may be regarded as the natural frequency of the j -th oscillator. The function $\Gamma_{jk}(\theta)$, known as the phase coupling function, represents the effect of the k -th oscillator on the j -th one when averaged over one period of limit-cycle oscillations of the common dynamics.

In the particular case when the function $G_{j\alpha, k\beta}$ is the same for all pairs (j, k) of oscillators, and has a magnitude of order $1/N$, Eq. (15) reduces to the form

$$\frac{d\theta_j}{dt} = \omega_j + \frac{\varepsilon}{N} \sum_{k=1, k \neq j}^N \Gamma(\theta_j - \theta_k). \quad (16)$$

The choice $\Gamma(\theta) = -\mathcal{K} \sin \theta$, with \mathcal{K} being a constant, reduces Eq. (16) to the dynamics of the celebrated Kuramoto model of synchronization [12, 17, 18, 19, 20, 21]:

$$\frac{d\theta_j}{dt} = \omega_j - \frac{K}{N} \sum_{k=1}^N \sin(\theta_j - \theta_k), \quad (17)$$

where we have defined $K \equiv \varepsilon \mathcal{K}$. The sine function in the last equation automatically takes care of the fact that the summation on the rhs does not include the term $k = j$. Moreover, the factor $1/N$ on the rhs ensures that the net effect felt by one oscillator due to all the other oscillators is

independent of their total number, thereby ensuring a well-defined behavior of the dynamics in the thermodynamic limit $N \rightarrow \infty$. The constant K characterizes the strength of coupling between the oscillators. While in this work, we will discuss the version of the Kuramoto model as in Eq. (17) that involves time-independent couplings, may we point out recent works of interest, Refs. [22, 23], on non-autonomous dynamics and time-varying frequencies and couplings in the framework of the Kuramoto model.

3. Synchronization in the Kuramoto model and the associated phase transition

The Kuramoto model is a dynamical system with N interacting degrees of freedom, and, as we will stress in the following, its invariant measure in the thermodynamic limit $N \gg 1$ may be quite effectively studied by using tools of statistical physics. In this limit, let $\mathcal{G}(\omega)$ be the normalized number density of the oscillator frequencies, i.e., the product $\mathcal{G}(\omega)d\omega$ gives the number of oscillators whose natural frequencies lie in the range $[\omega, \omega + d\omega]$, with $\int d\omega \mathcal{G}(\omega) = 1$. In the language of statistical physics, the ω_j 's may be regarded as random variables sampled from the underlying distribution $\mathcal{G}(\omega)$. Since the natural frequencies for a set of oscillators have given values that are time independent, ω_j 's are to be regarded as *quenched disordered* random variables, that is, those having values that do not evolve in time. This may be contrasted with *annealed disorder* associated with random variables whose values evolve in time.

The Kuramoto model has been mostly studied for a unimodal $\mathcal{G}(\omega)$ with a non-compact support, that is, one which is defined in the range $\omega \in [-\infty, \infty]$ and is symmetric about the mean $\langle \omega \rangle \equiv \int_{-\infty}^{\infty} d\omega \omega \mathcal{G}(\omega)$, and which decreases monotonically and continuously to zero with increasing $|\omega - \langle \omega \rangle|$. Of course, we assume here that $\mathcal{G}(\omega)$ is such that its mean exists and is finite. In this work, we will consider a $\mathcal{G}(\omega)$ that has all the aforementioned properties.

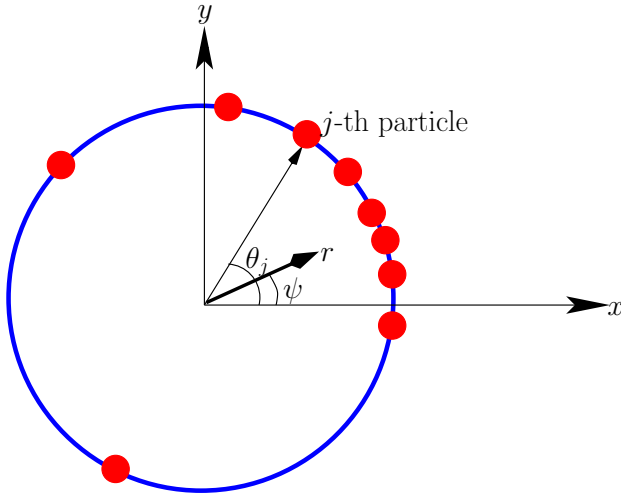


Figure 3. For the Kuramoto model of oscillators, Eq. (17), the figure shows the quantities r and ψ , see Eq. (18), for a given configuration of oscillator angles θ_j . As shown here, the centroid of the oscillator angles is given by the complex number $re^{i\psi}$.

In the dynamics (17), although a pair of oscillators is interacting rather weakly with one another due to the scaling of the coupling K by N , every oscillator is effectively responding to the *collective* influence of all the other oscillators. To see this, it is convenient to think of the oscillator angles as a collection of points moving on a unit circle. Then, at any time t , one may associate a vector of unit length to each point, take a vector sum, and divide by N , to get a vector of length $r(t)$

inclined at an angle $\psi(t)$ with respect to a reference axis [17, 18]:

$$r(t)e^{i\psi(t)} = \frac{1}{N} \sum_{j=1}^N e^{i\theta_j(t)}. \quad (18)$$

Here, $\psi(t)$ gives the average angle, while $r(t)$ measures the amount of phase coherence or synchrony in the system at time t , see Fig. 3. Indeed, if the angles are scattered around randomly on the circle, one has $r(t) = 0$, while, by contrast, if the oscillator angles are clustered together on the circle, we have $r(t) > 0$. In the extreme case when all the oscillator angles have the same value, $r(t)$ attains its maximum possible value of unity. Referring to Fig. 3, we may express the quantity r in terms of its x and y components as

$$\begin{aligned} r_x(t) &= \frac{1}{N} \sum_{j=1}^N \cos(\theta_j(t)) = r(t) \cos \psi(t), \\ r_y(t) &= \frac{1}{N} \sum_{j=1}^N \sin(\theta_j(t)) = r(t) \sin \psi(t), \\ r(t) &= \sqrt{r_x^2(t) + r_y^2(t)}, \quad \psi(t) = \tan^{-1}(r_y(t)/r_x(t)). \end{aligned} \quad (19)$$

In terms of $r(t)$ and $\psi(t)$, one may rewrite Eq. (17) as

$$\frac{d\theta_j}{dt} = \omega_j - Kr(t) \sin(\theta_j - \psi(t)), \quad (20)$$

which puts in evidence the fact that every oscillator is being influenced by the same combined effect expressed by the quantities $r(t)$ and $\psi(t)$ generated due to all the oscillators. Such a feature is generic to statistical physical models with the so-called mean-field interaction in which every constituent particle interacts with all the other particles with the same strength. The form (20) makes this mean-field nature of the dynamics evidently manifest.

In passing, let us make a relevant observation. Let us consider Eq. (17) and sum both sides over j . We get

$$\frac{d(1/N) \sum_{j=1}^N \theta_j}{dt} = \frac{1}{N} \sum_{j=1}^N \omega_j, \quad (21)$$

which implies that considering the swarm of angle points moving on the unit circle, their centroid turns around uniformly in time with a frequency equal to $(1/N) \sum_{j=1}^N \omega_j$ with respect to an inertial frame. In the limit $N \rightarrow \infty$, the quantity $(1/N) \sum_{j=1}^N \omega_j$ coincides with the mean $\langle \omega \rangle$ of the distribution $\mathcal{G}(\omega)$, by virtue of the law of large numbers. Note that for asymmetric unimodal frequency distribution (the case we do not consider in this work), the frequency with which the centroid turns around in time does not coincide with the mean of the frequency distribution [24].

From Eq. (20), we may easily understand the tendencies of the two terms on the rhs of the equation in dictating the behavior of the angles. The first term alone induces every oscillator to oscillate at its own natural frequency independently of the others, thereby promoting an unsynchronized state. By contrast, the mean-field term alone promotes synchrony, as may be seen

in the following way. Suppose at some instant of time t , a few of the oscillator angles happen to come close together on the circle, so that $r(t)$ and $\psi(t)$ have non-zero values. The dynamics $d\theta_j/dt = -Kr(t)\sin(\theta_j - \psi(t))$, which has a fixed point at $\theta_j = \psi(t)$, would then tend to pull the θ_j 's toward the instantaneous average angle $\psi(t)$. However, the effectiveness with which the θ_j 's are pulled toward $\psi(t)$ is proportional to the instantaneous amount of synchrony $r(t)$ present in the system, a feature that leads to a positive feedback loop being set up between coupling and synchrony: as more and more oscillators are pulled toward the instantaneous average angle, the value of r , and, consequently, the effective pull strength Kr grows, which in turn results in even more oscillators being pulled into the synchronized bunch. The process continues if further synchrony is promoted by more oscillators joining the synchronized bunch, or else, the process becomes self-limiting in time. The competing tendencies of the natural frequency and the mean-field term may be best inferred from numerical simulation results of the dynamics (20) for finite but large N . Simulations for a given unimodal $\mathcal{G}(\omega)$ reveal that for values of K less than a critical value K_c , the quantity $r(t)$ while starting from any initial condition decays at long times to a time-independent value equal to zero, with fluctuations of $O(N^{-1/2})$. For $K > K_c$, however, $r(t)$ grows exponentially in time to a time-independent value that is non-zero, still with fluctuations of order $N^{-1/2}$ [18].

The above-mentioned results make us conclude that the dynamics (20) leads at long times to a stationary state in which both r and ψ attain time-independent values, which we denote by r_{st} and ψ_{st} , respectively. Moreover, for a given $\mathcal{G}(\omega)$, qualitatively different stationary-state behavior emerges as K is tuned from small to high values across K_c : Small $K < K_c$ (respectively, large $K > K_c$) promotes an incoherent (respectively, a synchronized) stationary state. An unsynchronized/incoherent/homogeneous stationary state implies having the oscillator angles remaining scattered around randomly on the circle at all times, resulting in the value $r_{\text{st}} = 0$. A synchronized stationary state implies having a set of oscillator angles differing from one another by time-independent constant values so that the corresponding population moves around the circle in one compact bunch, and one has $r_{\text{st}} > 0$. In the case when one has a macroscopic population of $O(N)$ of synchronized oscillators, we may conclude by invoking the line of argument mentioned following Eq. (21) that the synchronized bunch moves around the unit circle with uniform frequency $\langle\omega\rangle$. In the limit $K \rightarrow \infty$, there is only one such synchronized bunch (thus yielding $r_{\text{st}} = 1$), while the number of synchronized oscillators steadily decreases to zero as K decreases towards K_c .

Now, in the language of statistical physics, the observation of qualitatively different macroscopic behaviors on tuning of a control parameter is referred to as a phase transition, a phenomenon that may be argued to be possible only in the thermodynamic limit [25]. At a quantitative level, a phase transition is characterized by different values of the so-called order parameter, which usually varies between zero in one phase and nonzero in the other. In the context of the Kuramoto model, the quantity r_{st} plays the role of an order parameter. For $K < K_c$ (respectively, $K > K_c$), one has a homogeneous (respectively, a synchronized) phase characterized by $r_{\text{st}} = 0$ (respectively, $r_{\text{st}} > 0$). On tuning K across K_c , one observes a second-order or a continuous phase transition, characterized by a continuous increase of r_{st} from zero as K is increased beyond K_c [18, 19]. The phase transition in the Kuramoto model for a unimodal $\mathcal{G}(\omega)$ is shown schematically in Fig. 4.

3.1. Analysis in the thermodynamic limit

In this section, we discuss the analytical properties of the Kuramoto model (20) in the thermodynamic limit $N \rightarrow \infty$. Before proceeding, let us note that the effect of $\langle\omega\rangle$ can be gotten rid of from the dynamics (20) by viewing the latter in a frame that is rotating uniformly with frequency $\langle\omega\rangle$ with respect to an inertial frame; this is tantamount to implementing the Galilean shift $\theta_j \rightarrow \theta_j + \langle\omega\rangle t \forall j$ that leaves the dynamics invariant. In the following, we will implement such a transformation, and consider from now on the ω_j 's to be random variables distributed according to

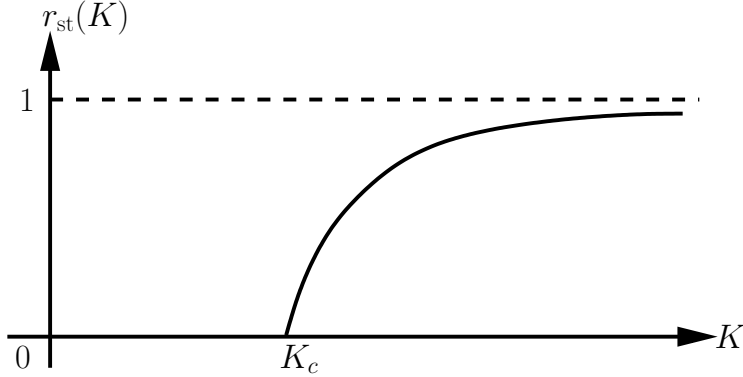


Figure 4. The figure shows the schematic dependence of the stationary-state order parameter r_{st} on the coupling strength K for the Kuramoto dynamics (20), with number of oscillators equal to N , and with a unimodal $\mathcal{G}(\omega)$ that has a non-compact support. The figure shows the behavior in the thermodynamic limit $N \rightarrow \infty$, when it is known that the Kuramoto model admits a second-order phase transition at the critical coupling strength K_c .

the distribution $g(\omega) \equiv \mathcal{G}(\omega + \langle \omega \rangle)$ with zero mean; note that $g(\omega) = g(-\omega)$. In this way of looking at things from the rotating frame, a macroscopic number of oscillators that are synchronized would have angle points that are immobile on the unit circle, while oscillators that are out of synchrony would have angle points going around the unit circle in time. Note that the dynamics (20) has now only two dynamical parameters: the width $\sigma \equiv \langle \omega^2 \rangle - \langle \omega \rangle^2$ of $g(\omega)$, which characterizes how different the individual natural frequencies are, and the coupling strength K , which characterizes how strongly the oscillators are affecting the motion of each other.

In the thermodynamic limit, it is natural to characterize the Kuramoto system in terms of a single-oscillator probability density $\rho(\theta, \omega, t)$ defined such that $\rho(\theta, \omega, t)d\theta$ gives the fraction of oscillators with natural frequency ω that have their angle lying between θ and $\theta + d\theta$ at time t [18, 19]. Note that invoking the concept of a probability density to describe a collection of dynamical variables and studying the time evolution of the density due to the dynamics of the dynamical variables is an approach adopted in statistical physics to analyze the dynamical behavior of a system. This approach may be contrasted with the one invoked in dynamical system theory, where instead one studies the time evolution of individual dynamical equations (for example, the set of coupled equations (20)) for given initial values of the dynamical variables.

The density ρ is non-negative, 2π -periodic in θ , and satisfies the normalization $\int_{-\pi}^{\pi} d\theta \rho(\theta, \omega, t) = 1 \forall \omega, t$. Since the total number of oscillators with a given natural frequency ω is conserved by the dynamics (20), the time evolution of ρ follows a continuity equation that may be derived by considering a small segment between θ and $\theta + \Delta\theta$ on the unit circle and oscillators with natural frequency equal to ω . Then, one may equate the change in a small time Δt the number of oscillator angle points contained in the segment, given by $\Delta\theta [\rho(\theta, \omega, t + \Delta t) - \rho(\theta, \omega, t)]$, with the net number of angle points that have entered the segment in time Δt , given by $[J(\theta, \omega, t) - J(\theta + \Delta\theta, \omega, t)] \Delta t$. Here, $J(\theta, \omega, t) = v(\theta, \omega, t)\rho(\theta, \omega, t)$ is the current at location θ at time t , with $v(\theta, \omega, t)$ being the local velocity at position θ . From Eq. (20), we have $v(\theta, \omega, t) = \omega - Kr(t) \sin(\theta - \psi(t))$, where the relation

$$r(t)e^{i\psi(t)} = \int_{-\infty}^{\infty} d\omega \int_{-\pi}^{\pi} d\theta g(\omega)\rho(\theta, \omega, t)e^{i\theta} \quad (22)$$

is obtained as the $N \rightarrow \infty$ generalization of Eq. (18). Realizing that the equality $\Delta\theta [\rho(\theta, \omega, t + \Delta t) - \rho(\theta, \omega, t)] = [J(\theta, \omega, t) - J(\theta + \Delta\theta, \omega, t)] \Delta t$ holds for arbitrary $\Delta\theta$, we get in

the limit $\Delta t \rightarrow 0$ the continuity equation $\partial\rho(\theta, \omega, t)/\partial t + \partial(v(\theta, \omega, t)\rho(\theta, \omega, t))/\partial\theta = 0$, i.e.,

$$\frac{\partial\rho}{\partial t} + \frac{\partial}{\partial\theta} \left[\left(\omega + K \int_{-\infty}^{\infty} \int_{-\pi}^{\pi} d\theta' \sin(\theta' - \theta) g(\omega) \rho(\theta', \omega, t) \right) \rho \right] = 0. \quad (23)$$

A stationary state of the dynamics (20) would mean to have a density such that $\partial\rho(\theta, \omega, t)/\partial t = 0$, that is, a time-independent density $\rho_{\text{st}}(\theta, \omega)$ that satisfies

$$\frac{\partial}{\partial\theta} \left[\left(\omega + K \int_{-\infty}^{\infty} \int_{-\pi}^{\pi} d\theta' \sin(\theta' - \theta) g(\omega) \rho_{\text{st}}(\theta', \omega) \right) \rho_{\text{st}}(\theta, \omega) \right] = 0. \quad (24)$$

Note that a state is to be considered stationary only in the statistical sense: in such a state, although individual oscillators continue to change their angles in accordance with the dynamics

$$\frac{d\theta_j}{dt} = \omega_j - Kr_{\text{st}} \sin(\theta_j - \psi_{\text{st}}), \quad (25)$$

the number of oscillators with a given value of the angle is constant in time. In Eq. (25), we may set ψ_{st} to zero by choosing suitably the origin of the angle axis, see Fig. 3. Such a choice would correspond to having the stationary values $r_{y,\text{st}} = 0$ and $r_{x,\text{st}} = r_{\text{st}}$, see Eq. (19). Consequently, one has

$$r_{\text{st}} = \int_{-\infty}^{\infty} d\omega \int_{-\pi}^{\pi} d\theta g(\omega) \rho_{\text{st}}(\theta, \omega) \cos\theta. \quad (26)$$

In his early works, Kuramoto adduced a remarkable analysis to predict the critical value K_c such that $r_{\text{st}} = 0$ for $K \leq K_c$ and $r_{\text{st}} > 0$ for $K > K_c$ [12]. The analysis cleverly bypasses the formidable task of solving explicitly Eq. (24). His prediction for K_c , borne out by later investigations, was

$$K_c = \frac{2}{\pi g(0)}. \quad (27)$$

We now recall the analysis due to Kuramoto [12, 18], which relies on adopting the following strategy well-known from statistical mechanical treatment of mean-field models [25]. At a fixed K , we first assume a given value of r_{st} , then (i) obtain the stationary density $\rho_{\text{st}}(\theta, \omega)$ implied by the stationary-state dynamics (25), and finally, (ii) require that the obtained density when substituted in Eq. (26) reproduces the given value of r_{st} , thereby yielding a self-consistent equation.

For a given value of r_{st} , it follows from Eq. (25) (with $\psi_{\text{st}} = 0$) that the dynamics of oscillators with $|\omega_j| \leq Kr_{\text{st}}$ approaches in time a stable fixed point defined by $\omega_j = Kr_{\text{st}} \sin\theta_j$, so that the j -th oscillator in this group has after evolving for a short time a time-independent angle given by $\theta_j = \sin^{-1}[\omega_j/(Kr_{\text{st}})]$; $|\theta_j| \leq \pi/2$. This group of oscillators is thus “locked” or synchronized, and has the density

$$\rho_{\text{st}}(\theta, \omega) = Kr_{\text{st}} \cos\theta \delta(\omega - Kr_{\text{st}} \sin\theta) \Theta(\cos\theta); \quad |\omega| \leq Kr_{\text{st}}, \quad (28)$$

where $\Theta(\cdot)$ is the Heaviside step function, and the prefactor is derived by the normalization condition $\int_{-\pi}^{\pi} d\theta \rho_{\text{st}}(\theta, \omega) = 1$. Equation (25) implies that oscillators with $|\omega_j| \geq Kr_{\text{st}}$ would however have ever drifting time-dependent angles. On the unit circle, the corresponding angle points would be buzzing around the circle, spending naturally longer duration at locations that allow for a smaller local velocity $v(\theta, \omega, t)$ and zipping through locations that have a larger local velocity. Consequently,

the density of this group of “drifting” oscillators would for most times be peaked around locations with small local velocities, thus leading to a stationary density for this group that is inversely proportional to the local velocity:

$$\rho_{\text{st}}(\theta, \omega) = \frac{C}{|\omega - Kr_{\text{st}} \sin \theta|}; \quad |\omega| > Kr_{\text{st}}. \quad (29)$$

Using the normalization condition $\int_{-\pi}^{\pi} d\theta \rho_{\text{st}}(\theta, \omega) = 1$, we get $C = (1/(2\pi))\sqrt{\omega^2 - (Kr_{\text{st}})^2}$.

We now require that the given value of r_{st} coincides with the one implied by Eq. (26) and the densities in Eqs. (28) and (29). Plugging the latter forms in Eq. (26), we get

$$\begin{aligned} r_{\text{st}} = & \int_{-\pi}^{\pi} d\theta \int_{|\omega| > Kr_{\text{st}}} d\omega g(\omega) \frac{C \cos \theta}{|\omega - Kr_{\text{st}} \sin \theta|} \\ & + \int_{-\frac{\pi}{2}}^{\frac{\pi}{2}} d\theta \int_{|\omega| \leq Kr_{\text{st}}} d\omega g(\omega) \cos \theta Kr_{\text{st}} \cos \theta \delta(\omega - Kr_{\text{st}} \sin \theta). \end{aligned} \quad (30)$$

The first integral on the rhs vanishes due to the symmetry $g(\omega) = g(-\omega)$ and the property that $\rho_{\text{st}}(\theta + \pi, -\omega) = \rho_{\text{st}}(\theta, \omega)$ for the group of drifting oscillators, as given by Eq. (29). The second integral after integration over ω yields the desired self-consistent equation

$$r_{\text{st}} = Kr_{\text{st}} \int_{-\pi/2}^{\pi/2} d\theta \cos^2 \theta g(Kr_{\text{st}} \sin \theta). \quad (31)$$

This equation has the trivial solution $r_{\text{st}} = 0$ valid for any K , which corresponds to the incoherent state with density $\rho_{\text{st}}^{\text{inc}}(\theta, \omega) = 1/(2\pi) \forall \theta, \omega$. One also has a solution with $r_{\text{st}} \neq 0$ that satisfies

$$1 = K \int_{-\pi/2}^{\pi/2} d\theta \cos^2 \theta g(Kr_{\text{st}} \sin \theta), \quad (32)$$

which bifurcates continuously from the incoherent solution at the value $K = K_c$ obtained from the above equation on taking the limit $r_{\text{st}} \rightarrow 0^+$. Since for a unimodal $g(\omega)$, one has a negative second derivative at $\omega = 0$, i.e., $g''(0) < 0$, one finds by expanding the integrand in Eq. (32) as a powers series in r_{st} that the bifurcation in this case is supercritical. It may be shown that consistently with Fig. 4, a solution r_{st} of Eq. (32) exists for $K \geq K_c$, which equals 0 for $K = K_c$, and which increases with K and approaches unity as $K \rightarrow \infty$ [20].

The linear stability of the incoherent state $\rho_{\text{st}}^{\text{inc}}$ may be studied by expanding $\rho(\theta, \omega, t)$ as $\rho(\theta, \omega, t) = \rho_{\text{st}}^{\text{inc}}(\theta, \omega) + \epsilon e^{\lambda t} \delta\rho(\theta, \omega)$; $|\epsilon| \ll 1$ [18]. Here, the parameter λ determines the stability properties of the incoherent state: when λ has a positive (respectively, a negative) real part, the state is linearly stable (respectively, unstable), while a purely imaginary λ implies that the state is linearly neutrally stable. Further, noting that $\rho(\theta, \omega, t)$, and hence, $\delta\rho(\theta, \omega)$ is 2π -periodic in θ , a Fourier expansion yields $\delta\rho(\theta, \omega) = (\tilde{\delta\rho}(\omega)e^{i\theta} + \text{c.c.}) + \delta\rho^\perp(\theta, \omega)$, where c.c. stands for complex conjugate, while $\delta\rho^\perp(\theta, \omega)$ contains second and higher harmonics of θ . Substituting in Eq. (23), one obtains an equation linear in $\tilde{\delta\rho}(\omega)$, as $\tilde{\delta\rho}(\omega) = [K/(2(\lambda + i\omega))] \int_{-\infty}^{\infty} d\omega' \tilde{\delta\rho}(\omega')g(\omega')$. Multiplying both sides by $g(\omega)$, and then integrating over ω , one obtains the characteristic equation determining λ , as $1 = (K/2) \int_{-\infty}^{\infty} d\omega g(\omega)/(\lambda + i\omega)$. For our choice of $g(\omega)$ that is even in ω and nowhere increasing on $\omega \in [0, \infty)$, it may be shown that the characteristic equation has at most one solution for λ , which when it exists is necessarily real [18]. The characteristic equation consequently reads $1 = (K/2) \int_{-\infty}^{\infty} d\omega \lambda g(\omega)/(\lambda^2 + \omega^2)$, which implies that λ can never be negative, and hence, that

the incoherent stationary state can never be linearly stable but is either neutrally stable or unstable ! The boundary between the neutrally stable and the unstable behavior is obtained by letting $\lambda \rightarrow 0^+$ in the characteristic equation, thereby yielding the critical value K_c of Eq. (27), such that the state is neutrally stable (respectively, stable) for $K < K_c$ (respectively, for $K > K_c$). In the light of the fact that $r(t)$ is obtained as an integral over $\rho(\theta, \omega, t)$, see Eq. (22), the latter fact seems apparently inconsistent with the numerical observation mentioned previously that for $K < K_c$, the quantity $r(t)$ while starting from any initial condition decays at long times to a time-independent value equal to zero. Indeed, neutral stability of the incoherent state implies sustained oscillations of $r(t)$, and whose decay in time, as observed in simulations, is possible only if a damping mechanism is present in the dynamics of $r(t)$. It has been rather rigorously demonstrated that indeed such a mechanism is present as regards the time evolution of $r(t)$ that draws analogy, as far as its mathematical structure is concerned, with the phenomenon of Landau damping present in plasma systems. We refer the reader to Ref. [18] for a highly readable account of the phenomenon and its observation in the Kuramoto model.

3.2. Noisy Kuramoto model

A rather interesting generalization of the Kuramoto model was studied by Sakaguchi, who considered the situation in which the Kuramoto oscillators do not have natural frequencies that are constant in time but which undergo rapid stochastic fluctuations in time [26]. Thus, in this model, the natural frequency of the j -th oscillator is a random variable that varies in time (thus representing annealed disorder) about the average given by ω_j . Note that in the case of the noisy Kuramoto model, there are two sources of randomness and two kinds of averaging involved. The natural frequency of the j -th oscillator is an annealed-disordered random variable that fluctuates in time, with the time-average denoted by ω_j . The set $\{\omega_j\}_{1 \leq j \leq N}$, referring to the time-averaged natural frequency of all the oscillators, themselves represent a set of quenched-disordered random variables sampled from the distribution $g(\omega)$. As discussed previously, $g(\omega)$ is unimodal and symmetric about zero, and moreover, decreases monotonically and continuously to zero with increasing $|\omega|$. The governing equations of motion of the noisy Kuramoto model are [26]

$$\frac{d\theta_j}{dt} = \omega_j - Kr(t) \sin(\theta_j - \psi(t)) + \eta_j(t), \quad (33)$$

where $\eta_j(t)$ is a Gaussian, white noise satisfying

$$\langle \eta_j(t) \rangle = 0, \quad \langle \eta_j(t) \eta_k(t') \rangle = 2D \delta_{jk} \delta(t - t'), \quad (34)$$

where $D \geq 0$ is a parameter that characterizes noise strength. Here and in the following, we will use angular brackets to denote averaging over noise realizations.

Note that Eq. (33), which is a stochastic differential equation, has the form of a Langevin equation. The reader may recall that a Langevin equation describes the time evolution of a subset of degrees of freedom that are changing only slowly in comparison to the remaining degrees of freedom of a system [27]. In our case of coupled oscillators, we take the natural frequencies of the oscillators to be fluctuating about their average values on a much faster timescale than the one over which the angle θ_j 's are evolving, and it is the former fast variation that leads to the stochastic noise $\eta_j(t)$ in the equations of motion. Equation (33) being a representative Langevin dynamics may be studied by employing the corresponding tool of analysis usual in statistical physical studies, namely, the Fokker-Planck equation [27, 28] for the time evolution of the single-oscillator probability density $\rho(\theta, \omega, t)$ defined above. This equation may be derived straightforwardly for the dynamics (33), and

has the form

$$\frac{\partial \rho}{\partial t} = D \frac{\partial^2 \rho}{\partial \theta^2} - \frac{\partial}{\partial \theta} \left[\left(\omega + K \int_{-\infty}^{\infty} \int_{-\pi}^{\pi} d\theta' \sin(\theta' - \theta) g(\omega) \rho(\theta', \omega, t) \right) \rho \right] = 0. \quad (35)$$

For $D = 0$, the above equation reduces to the continuity equation of the Kuramoto model, Eq. (23), as it should. Sakaguchi extended the self-consistent analysis of the Kuramoto model presented above to address the issue of which critical value of K allows in the stationary state for a branch of synchronized states to bifurcate from an incoherent state. The critical value is obtained as [26, 20]

$$K_c(D) = 2 \left[\int_{-\infty}^{+\infty} d\omega \frac{g(D\omega)}{\omega^2 + 1} \right]^{-1}, \quad (36)$$

which as $D \rightarrow 0^+$ may be checked to correctly reduce to the expected answer, namely, $K_c(0^+)$ equals K_c given by Eq. (27). It may be shown that the incoherent stationary state $\rho_{\text{st}}^{\text{inc}}(\theta, \omega) = 1/(2\pi)$ is linearly stable under the dynamics (35) for $K < K_c(D)$ and is linearly unstable for $K > K_c(D)$. Consequently, for $K < K_c(D)$ (respectively, $K > K_c(D)$), one has a homogeneous (respectively, a synchronized) phase characterized by $r_{\text{st}} = 0$ (respectively, $r_{\text{st}} > 0$). On tuning K , one observes a continuous transition between the two phases at $K = K_c(D)$. Figure 5 shows the phase boundary given by $K_c(D)$ between the homogeneous and the synchronized phase.

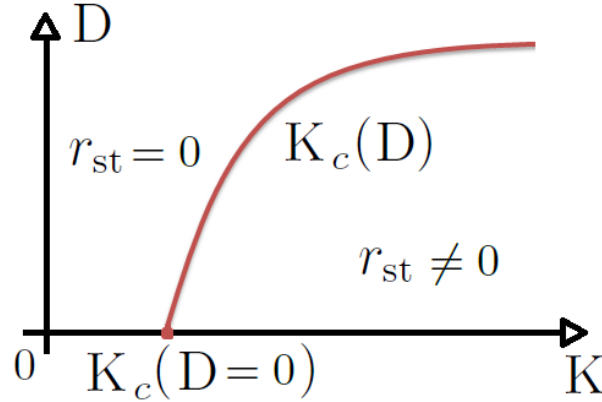


Figure 5. For the noisy Kuramoto model (33), the figure shows the phase boundary given by $K_c(D)$ between the homogeneous ($r_{\text{st}} = 0$) and the synchronized ($r_{\text{st}} > 0$) phase, with $K_c(D)$ given by Eq. (36).

4. Generalized Kuramoto model with inertia and noise

In this section, we study a very interesting generalization of the Kuramoto dynamics (20) that includes inertial terms parametrized by a moment of inertia and stochastic noise, as discussed in Refs. [29, 30, 31, 32, 33, 20]. Inclusion of inertia elevates the first-order Kuramoto dynamics to one that is second order in time, while noise accounts for temporal fluctuations of the natural frequencies. The generalization offers the possibility to explore the issue of emergence of spontaneous synchronization in a wider space of parameters, and, as we will discuss below, leads even with a unimodal natural frequency distribution to a rather rich phase diagram relative to the Kuramoto model that includes both equilibrium and nonequilibrium phase transitions. Besides, the generalized model represents a bridge between two apparently disconnected research areas, namely, the area

of spontaneous synchronization pursued by dynamical physicists and that of statistical physical studies, in both in and out of equilibrium regimes, of so-called long-range interacting systems pursued within the community of statistical physicists. It turns out that two different limits of the generalized model have been studied extensively over the years, albeit with not much overlap and inter-community dialogue, by the communities of dynamical and statistical physicists.

In the generalized dynamics, a dynamical variable in addition to the angle θ_j , namely, angular velocity v_j , is assigned to each oscillator, so that the equations of motion are [30, 31, 32]:

$$\frac{d\theta_j}{dt} = v_j, \quad m \frac{dv_j}{dt} = -\gamma v_j + \gamma \omega_j - \tilde{K} r \sin(\theta_j - \psi) + \tilde{\eta}_j(t). \quad (37)$$

Here, m is the common moment of inertia of the oscillators, $\gamma > 0$ is a parameter that plays the role of a damping constant, \tilde{K} is the strength of coupling between the oscillators, while $\tilde{\eta}_j(t)$ is a Gaussian, white noise satisfying

$$\langle \tilde{\eta}_j(t) \rangle = 0, \quad \langle \tilde{\eta}_j(t) \tilde{\eta}_k(t') \rangle = 2\tilde{D} \delta_{jk} \delta(t - t'). \quad (38)$$

Here, $\tilde{D} \geq 0$ is a parameter that sets the strength of the noise.

That γ plays the role of a damping constant in the dynamics (37) may be appreciated by considering the noise-average of the second equation in (37) that yields the dynamics $m d\langle v_j \rangle / dt = -\gamma \langle v_j \rangle + \gamma \omega_j - \tilde{K} \langle r \sin(\theta_j - \psi) \rangle$, which shows that in the absence of natural frequencies and the interaction between the oscillators, any average initial velocity decays to zero (natural frequencies and interaction would of course not let this happen!).

It is worth noting that the dynamics (37) without the noise term, studied in [29], arises in a completely different context, namely, in electrical power distribution networks comprising synchronous generators (representing power plants) and motors (representing customers) [10, 11]; the dynamics arises in the approximation in which every node of the network is connected to every other.

In the limit of overdamped motion ($m \rightarrow 0$ at a fixed $\gamma \neq 0$), the dynamics (37) reduces to

$$\gamma \frac{d\theta_j}{dt} = \gamma \omega_j - \tilde{K} r \sin(\theta_j - \psi) + \tilde{\eta}_j(t). \quad (39)$$

Then, defining $K \equiv \tilde{K}/\gamma$ and $\eta_j(t) \equiv \tilde{\eta}_j(t)/\gamma$ so that $D = \tilde{D}/\gamma^2$, the dynamics (39) for $D = 0$ becomes that of the Kuramoto model, Eq. (20), and for $D \neq 0$ that of its noisy version given by the dynamics (33).

4.1. The model as a long-range interacting system

It may be shown that in a different context than that of coupled oscillators, the dynamics (37) describes a long-range interacting system of particles moving on a unit circle, with each particle acted upon by a quenched external torque $\tilde{\omega}_j \equiv \gamma \omega_j$. Recent exploration of long-range interacting systems, and in particular, of their static and dynamic properties, has focussed on an analytically tractable and representative model called the Hamiltonian mean-field (HMF) model [13, 34].

Long-range interacting (LRI) systems are those in which the inter-particle interaction potential decays slower than $1/r^d$, with d being the dimension of the embedding space [35, 36, 37, 38, 39]. Unlike short-range ones, LRI systems are intrinsically nonadditive, namely, they cannot be trivially divided into independent macroscopic subparts. LRI systems are quite ubiquitous in Nature, typical examples being self-gravitating systems, charged plasmas, two-dimensional quasi-geostrophic flows, wave-particle interaction in plasma, etc. The feature of nonadditivity of LRI systems leads to many fascinating phenomena not exhibited by short-range systems, such as inequivalence of statistical

ensembles, breaking of ergodicity, occurrence of long-lived non-Boltzmann quasistationary states during relaxation to equilibrium, etc [37, 39].

The HMF model comprises N particles of mass m moving on a unit circle and interacting through a long-range interparticle potential that is of the mean-field type: every particle is coupled to every other with equal strength. The Hamiltonian of the HMF model is [13]

$$H = \sum_{j=1}^N \frac{p_j^2}{2m} + \frac{\tilde{K}}{2N} \sum_{j,k=1}^N [1 - \cos(\theta_j - \theta_k)], \quad (40)$$

where $\theta_j \in [-\pi, \pi]$ gives the position of the j -th particle on the circle, while $p_j = mv_j$ is its conjugated angular momentum, with v_j being the angular velocity. The time evolution of the system within a microcanonical ensemble follows the deterministic Hamilton equations of motion:

$$\frac{d\theta_j}{dt} = v_j, \quad m \frac{dv_j}{dt} = -\tilde{K}r \sin(\theta_j - \psi). \quad (41)$$

The dynamics conserves the total energy and momentum, and leads at long times to an equilibrium stationary state in which, depending on the energy density $\epsilon \equiv H/N$, the system could be in one of two possible phases: for ϵ smaller than a critical value $\epsilon_c = 3\tilde{K}/4$, the system is in a clustered phase in which the particles are close together on the circle, while for $\epsilon > \epsilon_c$, the particles are uniformly distributed on the circle, thus characterizing a homogeneous phase [35]. A continuous phase transition between the two phases is characterized by a positive value of r_{st} in the clustered phase and a zero value in the homogeneous phase.

One may generalize the microcanonical dynamics (41) to account for interaction with an external heat bath at temperature T . The resulting model, called the Brownian mean-field (BMF) model, has thus a canonical ensemble dynamics given by [40].

$$\frac{d\theta_j}{dt} = v_j, \quad m \frac{dv_j}{dt} = -\gamma v_j - \tilde{K}r \sin(\theta_j - \psi) + \tilde{\eta}_j(t), \quad (42)$$

where $\tilde{\eta}_j(t)$ is as in Eq. (38). One may then invoke the fluctuation-dissipation relation to express the strength \tilde{D} of the noise in terms of the temperature T and the damping constant γ as $\tilde{D} = \gamma k_B T$ [41]. We will set the Boltzmann constant k_B to unity in the rest of the paper. The canonical dynamics (42) also leads to a long-time equilibrium stationary state in which a generic configuration $C \equiv \{\theta_j, v_j\}_{1 \leq j \leq N}$ with energy $E(C)$ occurs with the usual Gibbs-Boltzmann weight: $P_{eq}(C) \propto \exp[-E(C)/T]$. The phase transition in the HMF model observed within the microcanonical ensemble now occurs within the canonical ensemble as one tunes the temperature across the critical value $T_c = \tilde{K}/2$. The derivation of this result is discussed below, namely, in Section 4.5.

Let us now consider a set of quenched external torques $\{\tilde{\omega}_j \equiv \gamma \omega_j\}$ acting on each of the particles, thereby pumping energy into the system. In this case, the second equation in the canonical dynamics (42) has an additional term $\tilde{\omega}_j$ on the rhs. The resulting dynamics becomes exactly the same as the dynamics (37) of the generalized Kuramoto model.

4.2. Dynamics in a reduced parameter space

It proves convenient to reduce the number of parameters in the dynamics (37). To this end, we note that the effect of σ may be made explicit by replacing ω_j in the second equation by $\sigma \omega_j$. Therefore, we will consider from now on the dynamics (37) with the substitution $\omega_j \rightarrow \sigma \omega_j$. In the resulting model, $g(\omega)$ therefore has zero mean and unit width. Moreover, we will consider in the dynamics

(37) the parameter \tilde{D} to be $\tilde{D} = \gamma T$, a relation we discussed above.

For $m \neq 0$, using dimensionless quantities [33, 20]

$$\bar{t} \equiv t\sqrt{\tilde{K}/m}, \quad \bar{v}_j \equiv v_j\sqrt{m/\tilde{K}}, \quad 1/\sqrt{\bar{m}} \equiv \gamma/\sqrt{\tilde{K}m}, \quad \bar{\sigma} \equiv \gamma\sigma/\tilde{K}, \quad \bar{T} \equiv T/\tilde{K}, \quad \bar{\eta}_j(\bar{t}) \equiv \tilde{\eta}_j(t)/\tilde{K}, \quad (43)$$

the equations of motion (37) become

$$\frac{d\theta_j}{d\bar{t}} = \bar{v}_j, \quad \frac{d\bar{v}_j}{d\bar{t}} = -\frac{1}{\sqrt{\bar{m}}}\bar{v}_j - r \sin(\theta_j - \psi) + \bar{\sigma}\omega_j + \bar{\eta}_j(\bar{t}), \quad (44)$$

where $\langle \bar{\eta}_j(\bar{t})\bar{\eta}_k(\bar{t}') \rangle = 2(\bar{T}/\sqrt{\bar{m}})\delta_{jk}\delta(\bar{t} - \bar{t}')$. For $m = 0$, using dimensionless time $\bar{t} \equiv t(\tilde{K}/\gamma)$, with $\bar{\sigma}$ and \bar{T} as defined above, the dynamics becomes the overdamped motion

$$\frac{d\theta_j}{d\bar{t}} = \bar{\sigma}\omega_j - r \sin(\theta_j - \psi) + \bar{\eta}_j(\bar{t}), \quad (45)$$

where we have $\langle \bar{\eta}_j(\bar{t})\bar{\eta}_k(\bar{t}') \rangle = 2\bar{T}\delta_{jk}\delta(\bar{t} - \bar{t}')$. We thus have in place of the dynamics (37) involving five parameters, $m, \gamma, \tilde{K}, \sigma, T$ the reduced dynamics (44) (or (45) in the overdamped limit) that involves three dimensionless parameters, $\bar{m}, \bar{T}, \bar{\sigma}$. We will from now on consider the dynamics in this reduced parameter space, dropping overbars for simplicity of notation. With $\sigma = 0$ (i.e. $g(\omega) = \delta(\omega)$) the dynamics (44) is that of the BMF model with an equilibrium stationary state. For other $g(\omega)$, it may be shown that the dynamics (44) violates detailed balance, leading to a NESS [33].

4.3. Nonequilibrium first-order synchronization phase transition

In this section, we report results on a very interesting nonequilibrium phase transition that occurs in the stationary state of the dynamics (44). In the three-dimensional space of parameters (m, T, σ) , let us first locate the phase transitions in the Kuramoto model, Eq. (20), and in its noisy extension, Eq. (33), respectively.

- The phase transition of the Kuramoto dynamics ($m = T = 0, \sigma \neq 0$) corresponds to a continuous transition from a low- σ synchronized to a high- σ incoherent phase across the critical point

$$\sigma_c(m = 0, T = 0) = \frac{\pi g(0)}{2}, \quad (46)$$

which is obtained using Eq. (27), see Ref. [20].

- Extending the Kuramoto dynamics to $T \neq 0$ (the noisy Kuramoto model), the aforementioned critical point becomes a second-order critical line on the (T, σ) -plane, given by solving

$$2 = \int_{-\infty}^{\infty} d\omega \frac{g(\omega)T}{T^2 + \omega^2\sigma_c^2(m = 0, T)}. \quad (47)$$

The above equation is obtained by using Eq. (36), as may be looked up in Ref. [20].

- The transition in the BMF dynamics ($m, T \neq 0, \sigma = 0$) corresponds now to a continuous transition occurring at the critical temperature $T_c = 1/2$. This result is proved in Section 4.5.

Figure 6(a) shows the complete phase diagram of the model (44), in which the thick red second-order critical lines denote the continuous transitions mentioned above [33, 20]. For m, σ, T all

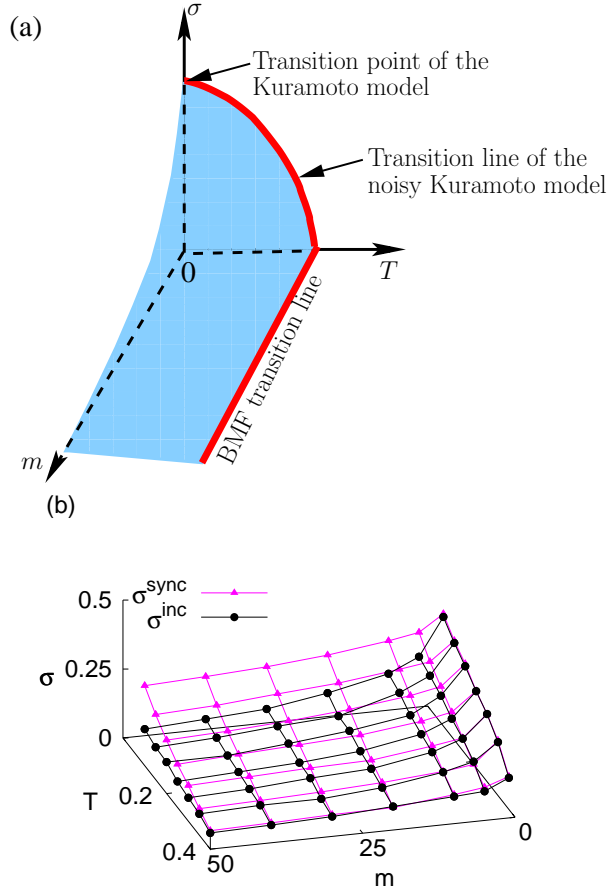


Figure 6. Panel (a) shows the schematic phase diagram of model (44) in the three-dimensional space of the parameters, the dimensionless moment of inertia m , the temperature T , and the width of the frequency distribution σ . The shaded blue surface is a first-order transition surface, and the thick red lines are second-order critical lines. The system is synchronized inside the region bounded by the surface, and is incoherent outside. The figure also shows the transitions of known models discussed in the text. The blue surface in (a) is bounded from above and below by the dynamical stability thresholds $\sigma^{\text{sync}}(m, T)$ and $\sigma^{\text{inc}}(m, T)$ of respectively the synchronized and the incoherent phase, which are estimated in N -body simulations from hysteresis plots (see Fig. 7 for an example). The surfaces $\sigma^{\text{sync}}(m, T)$ and $\sigma^{\text{inc}}(m, T)$ obtained in numerical simulations for $N = 500$ and with a Gaussian $g(\omega)$ with zero mean and unit width are shown in panel (b). <https://doi.org/10.1088/1742-5468/14/08/R08001> ©SISSA Medialab Srl. Reproduced by permission of IOP Publishing. All rights reserved.

non-zero, however, the synchronization transition becomes first order, occurring across the shaded blue transition surface. The surface is bounded by the second-order critical lines on the (T, σ) and (m, T) planes, and by a first-order transition line on the (m, σ) -plane. Let us remark that all phase transitions for $\sigma \neq 0$ are in NESSs.

The first-order nature of the phase transition becomes evident on analyzing results of N -body simulations of the dynamics (44) for a representative $g(\omega)$, for example, a Gaussian distribution $g(\omega) = \exp(-\omega^2/2)/\sqrt{2\pi}$ [33, 20]. For given values of m and T , an initial state, which has all the oscillators at $\theta = 0$ and angular velocities v_i 's sampled from a Gaussian distribution with zero mean and standard deviation $\propto T$, was first allowed to equilibrate at $\sigma = 0$. The state was subsequently allowed to evolve under the condition of σ increasing adiabatically to high values and back in a cycle. In Fig. 7(a), we show the behavior of r for several m 's at a fixed value of T smaller than the BMF transition point $T_c = 1/2$. In the figure, one may observe sharp jumps and hysteresis behavior reminiscent of a first-order transition. With decrease of m , one may observe that the jumps in r

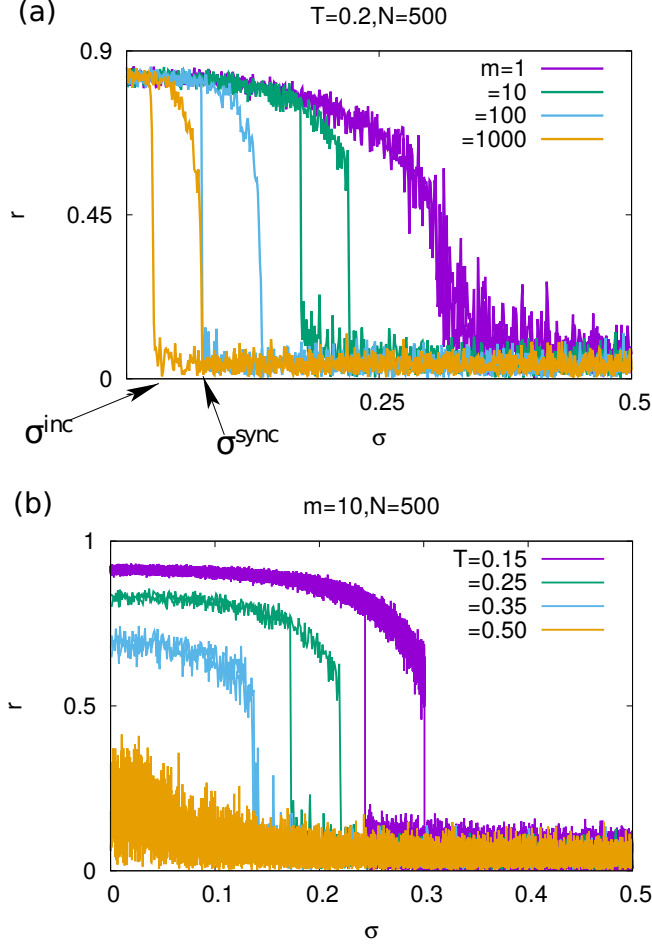


Figure 7. For the model (44), the figure shows (a) r vs. adiabatically-tuned σ for different values of m at $T = 0.2 < T_c = 1/2$ (with T_c being the BMF transition point), and also the stability thresholds, $\sigma^{\text{inc}}(m, T)$ and $\sigma^{\text{sync}}(m, T)$, for $m = 1000$, and (b) r vs. adiabatically tuned σ for different temperatures $T \leq T_c = 1/2$ at a fixed moment of inertia $m = 10$. For a given m in (a), the branch of the plot to the right (left) corresponds to σ increasing (decreasing); for $m = 1$, the two branches almost overlap. For a given T in (b), the branch of the plot to the right (left) corresponds to σ increasing (decreasing); for $T \geq 0.45$, the two branches practically overlap. The data are obtained from numerical integration of the dynamics (44) for $N = 500$ and a Gaussian $g(\omega)$ with zero mean and unit width. <https://doi.org/10.1088/1742-5468/14/08/R08001> ©SISSA Medialab Srl. Reproduced by permission of IOP Publishing. All rights reserved.

become less sharp, and the hysteresis loop area decreases, both features being consistent with the fact that the transition becomes second-order-like as $m \rightarrow 0$, see Fig. 6(a). For $m = 1000$, we show in Fig. 7(a) the approximate stability thresholds for the incoherent and the synchronized state, which are denoted respectively by $\sigma^{\text{inc}}(m, T)$ and $\sigma^{\text{sync}}(m, T)$. The actual phase transition point $\sigma_c(m, T)$ lies in between the two thresholds. Let us note from the figure that both the thresholds decrease and approach zero with the increase of m . Figure 7(b) shows hysteresis plots for a Gaussian $g(\omega)$ at a fixed m and for several values of $T \leq T_c$: one observes that with T approaching T_c , the hysteresis loop area decreases, jumps in r become less sharp and occur between smaller and smaller values that approach zero. Moreover, the r value at $\sigma = 0$ decreases as T increases towards T_c , reaching zero at T_c . These findings imply that the thresholds $\sigma^{\text{inc}}(m, T)$ and $\sigma^{\text{sync}}(m, T)$ coincide on the second-order critical lines, as expected, and moreover, they come asymptotically close together and approach zero in the limit $m \rightarrow \infty$ at a fixed T . For given values of m and T and σ in the range $\sigma^{\text{inc}}(m, T) < \sigma < \sigma^{\text{sync}}(m, T)$, we show in Fig. 8(a) the quantity r as a function of time in the

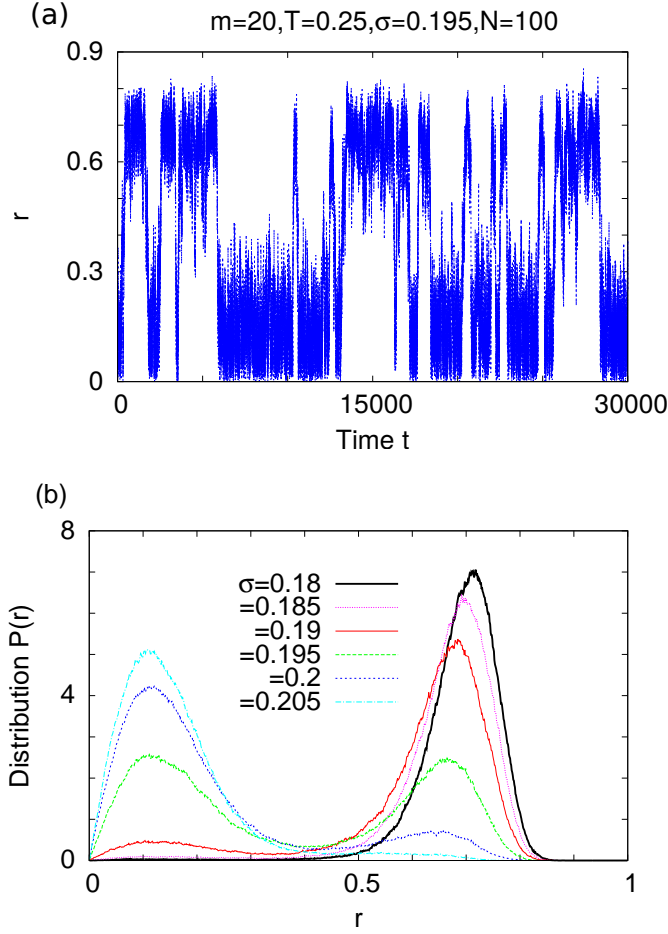


Figure 8. For the dynamics (44) at $m = 20, T = 0.25, N = 100$, and for a Gaussian $g(\omega)$ with zero mean and unit width, panel (a) shows at $\sigma = 0.195$, which is the numerically estimated first-order phase transition point, the quantity r as a function of time in the stationary state, while panel (b) shows the distribution $P(r)$ at several σ 's around 0.195. The data are obtained from numerical integration of the dynamical equations (44) with $N = 100$. <https://doi.org/10.1088/1742-5468/14/08/R08001> ©SISSA Medialab Srl. Reproduced by permission of IOP Publishing. All rights reserved.

stationary state. One may observe from the figure a bistable behavior, with the system switching back and forth between incoherent ($r \approx 0$) and synchronized ($r > 0$) states. Consistently, the distribution $P(r)$ shown in Figure 8(b) is indeed bimodal with a peak around either $r \approx 0$ or $r > 0$ as σ varies between $\sigma^{\text{inc}}(m, T)$ and $\sigma^{\text{sync}}(m, T)$. Figure 8 lends further evidence in support of the phase transition being first order [42].

4.4. Analysis in the continuum limit: The Kramers equation

In this section, we discuss analytical characterization of the dynamics (44) in the continuum limit $N \rightarrow \infty$. Similar to what was done for the Kuramoto model, we define a single-oscillator density $f(\theta, v, \omega, t)$ that gives at time t and for each ω the fraction of oscillators that have angle θ and angular velocity v . The density f is 2π -periodic in θ , obeys the normalization $\int_{-\pi}^{\pi} d\theta \int_{-\infty}^{+\infty} dv f(\theta, v, \omega, t) =$

$1 \forall \omega, t$, and has a time evolution given by the so-called Kramers equation [28, 32, 33, 20]

$$\frac{\partial f}{\partial t} = -v \frac{\partial f}{\partial \theta} + \frac{\partial}{\partial v} \left(\frac{v}{\sqrt{m}} - \sigma \omega + r \sin(\theta - \psi) \right) f + \frac{T}{\sqrt{m}} \frac{\partial^2 f}{\partial v^2}, \quad (48)$$

with $r(t)e^{i\psi(t)} = \int d\theta dv d\omega g(\omega) e^{i\theta} f(\theta, v, \omega, t)$.

We are interested in the stationary state solutions of the Kramers equation, obtained by setting the left hand side of Eq. (48) to zero. As already mentioned, the stationary state is a NESS, unless $\sigma = 0$. In the stationary state, the quantities r and ψ have their stationary-state values r_{st} and ψ_{st} , respectively. The stationary-state single-oscillator density $f_{\text{st}}(\theta, v, \omega)$ thus satisfies

$$0 = -v \frac{\partial f_{\text{st}}}{\partial \theta} + \frac{\partial}{\partial v} \left(\frac{v}{\sqrt{m}} - \sigma \omega + r_{\text{st}} \sin(\theta - \psi_{\text{st}}) \right) f_{\text{st}} + \frac{T}{\sqrt{m}} \frac{\partial^2 f_{\text{st}}}{\partial v^2}. \quad (49)$$

Similar to what was done in Section 3.1, we may set ψ_{st} to zero by choosing suitably the origin of the angle axis, which corresponds to having the stationary values $r_{y,\text{st}} = 0$ and $r_{x,\text{st}} = r_{\text{st}}$, see Eq. (19). Consequently, one has

$$r_{\text{st}} = \int d\theta dv d\omega g(\omega) \cos \theta f_{\text{st}}(\theta, v, \omega). \quad (50)$$

From now on, we will consider the stationary-state Kramers equation with $\psi_{\text{st}} = 0$.

4.5. $\sigma = 0$: Stationary solutions and the associated phase transition

For $\sigma = 0$, the stationary-state single-oscillator density is given by the Gibbs-Boltzmann measure corresponding to canonical equilibrium [20]:

$$f_{\text{st}}(\theta, v) = \frac{\exp[-v^2/(2T) + (r_{\text{st}}/T) \cos \theta]}{\sqrt{2\pi T} \int_{-\pi}^{\pi} d\theta \exp[(r_{\text{st}}/T) \cos \theta]}, \quad (51)$$

where the denominator is the normalization factor that ensures that $\int_{-\infty}^{\infty} dv \int_{-\pi}^{\pi} d\theta f_{\text{st}}(\theta, v) = 1$. One may easily check by direct substitution that the above form¹ satisfies Eq. (49) with $\sigma = 0$ and with $\psi_{\text{st}} = 0$. Using Eqs. (50) and (51), we get

$$r_{\text{st}} = \int d\theta dv \cos \theta f_{\text{st}}(\theta, v) = \frac{\int_{-\pi}^{\pi} d\theta \cos \theta \exp[(r_{\text{st}}/T) \cos \theta]}{\int_{-\pi}^{\pi} d\theta \exp[(r_{\text{st}}/T) \cos \theta]}. \quad (52)$$

The self-consistency condition, Eq. (52), has a trivial solution $r_{\text{st}} = 0$ valid at all temperatures, while it may be shown that a non-zero solution exists for T smaller than a critical value $T_c = 1/2$ [35]. Reverting to dimensional temperatures by using Eq. (43), we obtain the critical temperature of the BMF model as $T_c = \tilde{K}/2$, as announced towards the end of Section 4.1.

¹Note that with $\sigma = 0$, all the oscillators have the same natural frequency equal to $\langle \omega \rangle$, and the need to group the oscillators based on their natural frequencies, as was done for defining the density $f(\theta, v, \omega, t)$, is no longer there. Consequently, one has the stationary-state single-oscillator density denoted by $f_{\text{st}}(\theta, v)$ and which is defined as the fraction of oscillators that have angle θ and angular velocity v in the stationary state.

4.6. $\sigma \neq 0$: Incoherent stationary state and its linear stability

For $\sigma \neq 0$, the θ -independent solution characterizing the incoherent phase, for which $r_{\text{st}} = 0$, is given by [32]:

$$f_{\text{st}}^{\text{inc}}(\theta, v, \omega) = \frac{1}{2\pi} \sqrt{\frac{1}{2\pi T}} \exp \left[-\frac{(v - \sigma\omega\sqrt{m})^2}{2T} \right]. \quad (53)$$

The linear stability analysis of the incoherent state (53) may be carried out by expanding $f(\theta, v, \omega, t)$ as $f(\theta, v, \omega, t) = f_{\text{st}}^{\text{inc}}(\theta, v, \omega) + e^{\lambda t} \delta f(\theta, v, \omega)$, with $|\delta f| \ll 1$, substituting in Eq. (48), and keeping terms to linear order in δf . The solution of the linearized equation yields the following equation that λ has to satisfy [32]:

$$\frac{2T}{e^{mT}} = \sum_{p=0}^{\infty} \frac{(-mT)^p (1 + \frac{p}{mT})}{p!} \int_{-\infty}^{\infty} \frac{g(\omega) d\omega}{1 + \frac{p}{mT} + i\frac{\sigma\omega}{T} + \frac{\lambda}{T\sqrt{m}}}. \quad (54)$$

A rather long analysis allows one to prove that the above equation has one and only one solution for λ with a positive real part, and when this single solution exists, it is necessarily real [33, 20]. A positive (respectively, negative) λ implies that the incoherent state (53) is linearly unstable (respectively, stable). It then follows that at the point of neutral stability, one has $\lambda = 0$, which when substituted in Eq. (54) gives $\sigma^{\text{inc}}(m, T)$, the stability threshold of the incoherent stationary state, satisfying

$$\frac{2T}{e^{mT}} = \sum_{p=0}^{\infty} \frac{(-mT)^p (1 + \frac{p}{mT})^2}{p!} \int_{-\infty}^{\infty} \frac{g(\omega) d\omega}{(1 + \frac{p}{mT})^2 + \frac{(\sigma^{\text{inc}})^2 \omega^2}{T^2}}. \quad (55)$$

In the (m, T, σ) space, the above equation defines the stability surface $\sigma^{\text{inc}}(m, T)$. There will similarly be the stability surface $\sigma^{\text{sync}}(m, T)$ representing the stability threshold of the synchronized stationary state. The reader may refer to Fig. 6(b) that shows the two surfaces obtained in N -body simulations for $N = 500$ for a Gaussian $g(\omega)$.

The two surfaces, $\sigma^{\text{inc}}(m, T)$ and $\sigma^{\text{sync}}(m, T)$, coincide on the critical lines on the (T, σ) and (m, T) planes where the transition becomes continuous, while outside these planes, the surfaces enclose the first-order transition surface $\sigma_c(m, T)$, that is, $\sigma^{\text{sync}}(m, T) > \sigma_c(m, T) > \sigma^{\text{inc}}(m, T)$, see Fig. 6(a). In this regard, let us show by taking suitable limits that the surface $\sigma^{\text{inc}}(m, T)$ meets the critical lines on the (T, σ) and (m, T) planes. We will also obtain the intersection of this surface with the (m, σ) -plane. On considering $m \rightarrow 0$ at a fixed T , noting that only the $p = 0$ term in the sum in Eq. (55) contributes yields $\lim_{m \rightarrow 0, T \text{ fixed}} \sigma^{\text{inc}}(m, T) = \sigma_c(m = 0, T)$, with the implicit expression of $\sigma_c(m = 0, T)$ given by Eq. (47). One also finds that $\lim_{T \rightarrow T_c^-, m \text{ fixed}} \sigma^{\text{inc}}(m, T) = 0$, that

is, on the (m, T) plane, the transition line is given by $T_c = 1/2$. When $T \rightarrow 0$ at a fixed m , we get $\sigma_{\text{noiseless}}^{\text{inc}}(m) \equiv \lim_{T \rightarrow 0, m \text{ fixed}} \sigma^{\text{inc}}(m, T)$, with [33, 20].

$$1 = \frac{\pi g(0)}{2\sigma_{\text{noiseless}}^{\text{inc}}} - \frac{m}{2} \int_{-\infty}^{\infty} d\omega \frac{g(\omega)}{[1 + m^2(\sigma_{\text{noiseless}}^{\text{inc}})^2 \omega^2]}. \quad (56)$$

4.7. $\sigma \neq 0$: Synchronized stationary state

For $\sigma \neq 0$, the existence of the synchronized stationary state is borne out by our simulation results shown in Figs. 7 and 8. For general σ , we expand the single-oscillator density for the synchronized stationary state as [43]

$$f_{\text{st}}^{\text{sync}}(\theta, v, \omega) = \Phi_0 \left(\frac{v}{\sqrt{2T}} \right) \sum_{n=0}^{\infty} b_n(\theta, \omega) \Phi_n \left(\frac{v}{\sqrt{2T}} \right). \quad (57)$$

Here, the functions b_n satisfy $b_n(\theta, \omega) = b_n(\theta + 2\pi, \omega)$ to ensure that $f_{\text{st}}^{\text{sync}}$ is 2π -periodic in θ , while $\Phi_n(ax)$ is the Hermite function: $\Phi_n(ax) = \sqrt{a/(2^n n! \sqrt{\pi})} \exp\left[-\frac{a^2 x^2}{2}\right] H_n(ax)$, with $H_n(x)$'s being the n -th degree Hermite polynomial. The functions Φ_n are orthonormal: $\int dx \Phi_m(ax) \Phi_n(ax) = \delta_{mn}$. Normalization of $f_{\text{st}}^{\text{sync}}(\theta, v, \omega)$ implies the equality $\int_{-\pi}^{\pi} d\theta b_0(\theta, \omega) = 1$, while the self-consistent values of the parameters r_{st} are given by

$$r_{\text{st}} = \int d\omega g(\omega) \int_{-\pi}^{\pi} d\theta b_0(\theta, \omega) \cos \theta. \quad (58)$$

Furthermore, using $\int dx x \Phi_0(ax) \Phi_n(ax) = 1/(\sqrt{2}a) \delta_{n,1}$, we obtain that $\int dv v f_{\text{st}}^{\text{sync}}(\theta, v, \omega) = \sqrt{T} b_1(\theta, \omega)$. On the other hand, integrating over v the stationary-state Kramers equation (49), we obtain that $\int dv v f_{\text{st}}^{\text{sync}}(\theta, v, \omega)$ and, hence, $b_1(\theta, \omega)$, does not depend on θ . Choosing the Hermite functions in the expansion (57) is motivated by the fact that for $\sigma = 0$, the density $f_{\text{st}}^{\text{sync}}(\theta, v, \omega)$ has the Gibbs-Boltzmann form, $f_{\text{st}}^{\text{sync}}(\theta, v, \omega) \sim \exp[-v^2/(2T) + r_{\text{st}} \cos \theta]$, cf. Eq. (51). As may be shown [43], the expansion coefficients b_n for this case satisfy $b_0(\theta, 0) \sim \exp[r_{\text{st}} \cos \theta]$, $b_n(\theta, 0) = 0$ for $n > 0$, so that only the $n = 0$ term in the expansion (57) has to be taken into account; then, with $\Phi_0(x) \sim \exp(-x^2/2)$, the product $\Phi_0(v/\sqrt{2T}) \Phi_0(v/\sqrt{2T})$ appearing in the expansion correctly reproduces the velocity-part of the density $\sim \exp[-v^2/(2T)]$.

On plugging the expansion (57) into the stationary-state Kramers equation (49), on using the known recursion relations for the Hermite polynomials, and on equating to zero the coefficient of each Φ_n , we get [43]

$$\sqrt{nT} \frac{\partial b_{n-1}(\theta, \omega)}{\partial \theta} + \sqrt{(n+1)T} \frac{\partial b_{n+1}(\theta, \omega)}{\partial \theta} + \frac{n}{\sqrt{m}} b_n(\theta, \omega) + \sqrt{\frac{n}{T}} b_{n-1}(\theta, \omega) [r_{\text{st}} \sin \theta - \sigma \omega] = 0 \quad (59)$$

for $n = 0, 1, 2, \dots$ (with the understanding that $b_{-1}(\theta, \omega) \equiv 0$). The equation for $n = 0$ recovers the result that $b_1(\theta, \omega)$ is independent of θ . Noting the scaling of the various terms in Eq. (59) with m , we expand $b_n(\theta, \omega)$ as [43]

$$b_n(\theta, \omega) = \sum_{k=0}^{\infty} (\sqrt{m})^k c_{n,k}(\theta, \omega), \quad (60)$$

which may be shown to be an asymptotic expansion in \sqrt{m} [43], thus requiring a proper numerical evaluation of the sum on the rhs by invoking the so-called Borel summation method [44]. Now, using Eq. (60), we conclude that $b_1(\theta, \omega)$ being independent of θ implies that so is $c_{1,k}(\theta, \omega) \forall k$. The only constraint on $b_0(\theta, \omega)$ being $\int_{-\pi}^{\pi} d\theta b_0(\theta, \omega) = 1$, we may without loss of generality choose $c_{0,k \geq 1}(0, \omega) = 0$. We now use Eq. (60) in Eq. (59) and equate to zero the coefficient of each power

of \sqrt{m} . The term proportional to $(\sqrt{m})^{-1}$ gives simply $nc_{n,0}(\theta, \omega) = 0$, which implies that we have $c_{n,0}(\theta, \omega) = 0$ for $n > 0$. The coefficient of the term proportional to $(\sqrt{m})^k$ leads to [43]

$$\sqrt{nT} \frac{\partial c_{n-1,k}(\theta, \omega)}{\partial \theta} + \sqrt{(n+1)T} \frac{\partial c_{n+1,k}(\theta, \omega)}{\partial \theta} + \sqrt{nT} a(\theta, \omega) c_{n-1,k}(\theta, \omega) + nc_{n,k+1}(\theta, \omega) = 0 \quad (61)$$

for $n, k = 0, 1, 2, \dots$ (with $c_{-1,k}(\theta, \omega) \equiv 0$), where $a(\theta, \omega) \equiv [r_{\text{st}} \sin \theta - \sigma \omega]/T$. The system of equations (61) can be solved recursively. While the details of solving these equations may be found in Ref. [43], we quote here only the solutions:

$$c_{0,0}(\theta, \omega) = c_{0,0}(0, \omega) e^{-h(\theta, \omega)} \left[1 + \left(e^{h(2\pi, \omega)} - 1 \right) \frac{\int_0^\theta d\theta' e^{h(\theta', \omega)}}{\int_{-\pi}^\pi d\theta' e^{h(\theta', \omega)}} \right], \quad (62)$$

$$c_{1,1}(\omega) = \sqrt{T} \frac{c_{0,0}(0, \omega) (1 - e^{h(2\pi, \omega)})}{\int_{-\pi}^\pi d\theta' e^{h(\theta', \omega)}}, \quad (63)$$

$$c_{n,n}(\theta, \omega) = -\sqrt{\frac{T}{n}} \left[\frac{\partial c_{n-1,n-1}(\theta, \omega)}{\partial \theta} + a(\theta, \omega) c_{n-1,n-1}(\theta, \omega) \right], \quad (64)$$

$$c_{0,2k}(\theta, \omega) = \sqrt{2} \frac{\int_{-\pi}^\pi d\theta' \frac{\partial c_{2,2k}(\theta', \omega)}{\partial \theta'} e^{h(\theta', \omega)}}{\int_{-\pi}^\pi d\theta' e^{h(\theta', \omega)}} e^{-h(\theta, \omega)} \int_0^\theta d\theta' e^{h(\theta', \omega)} - \sqrt{2} e^{-h(\theta, \omega)} \int_0^\theta d\theta' \frac{\partial c_{2,2k}(\theta', \omega)}{\partial \theta'} e^{h(\theta', \omega)}, \quad (65)$$

$$c_{1,1+2k}(\omega) = -\sqrt{2T} \frac{\int_{-\pi}^\pi d\theta' \frac{\partial c_{2,2k}(\theta', \omega)}{\partial \theta'} e^{h(\theta', \omega)}}{\int_{-\pi}^\pi d\theta' e^{h(\theta', \omega)}}, \quad (66)$$

$$c_{2,2+2k}(\theta, \omega) = -\sqrt{\frac{T}{2}} a(\theta, \omega) c_{1,1+2k}(\omega) - \frac{\sqrt{3T}}{2} \frac{\partial c_{3,1+2k}(\theta, \omega)}{\partial \theta}, \quad (67)$$

$$c_{n,n+2k}(\theta, \omega) = -\sqrt{\frac{T}{n}} \left[\frac{\partial c_{n-1,n-1+2k}(\theta)}{\partial \theta} + a(\theta, \omega) c_{n-1,n-1+2k}(\theta, \omega) \right] - \frac{\sqrt{(n+1)T}}{n} \frac{\partial c_{n+1,n-1+2k}(\theta, \omega)}{\partial \theta} \quad n \geq 3, \quad (68)$$

with $k = 1, 2, \dots$. Here, we have defined $h(\theta, \omega) \equiv \int_0^\theta d\theta' a(\theta', \omega)$.

Figure 9 shows schematically the flow of the solution up to $n = k = 6$, while that for higher values proceeds analogously. As shown, the system (61) computes progressively each element of the main diagonal, and then the elements of the second upper diagonal, each one determined by the knowledge of two previously determined elements, and so on. Each element of the matrix is proportional to $c_{0,0}(0, \omega)$, which is fixed by the normalization of $f_{\text{st}}^{\text{sync}}$: $\sum_{k=0}^\infty \int_{-\pi}^\pi d\theta (\sqrt{m})^{2k} c_{0,2k}(\theta, \omega) = 1$. The values of r_{st} have to be determined self-consistently by using Eqs. (58) and (60).

For illustrating an application of the aforementioned scheme, let us choose a representative $g(\omega)$, namely, a Gaussian: $g(\omega) = 1/(\sqrt{2\pi}) \exp(-\omega^2/2)$, and obtain in the synchronized phase the marginal θ -distribution, $n(\theta) \equiv \int_{-\infty}^\infty d\omega g(\omega) \int_{-\infty}^\infty dv f_{\text{st}}^{\text{sync}}(\theta, v, \omega)$, and the quantity $p(\theta) \equiv \int_{-\infty}^\infty d\omega g(\omega) \int_{-\infty}^\infty dv v^2 f_{\text{st}}^{\text{sync}}(\theta, v, \omega)$ that is proportional to the local pressure [25]. Orthonormality

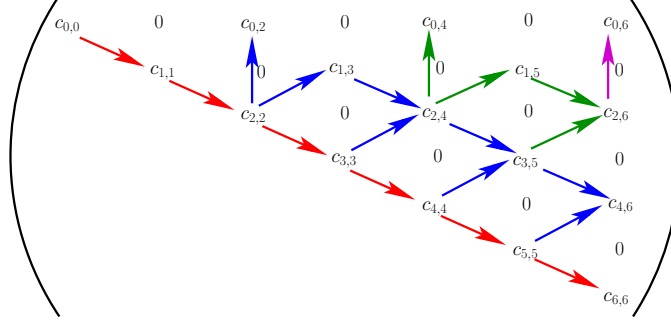


Figure 9. Flow diagram for the evaluation of the expansion coefficients $c_{n,k}(\theta, \omega)$; $n, k = 0, 1, 2, \dots, 6$ by using Eq. (61). Starting from the main diagonal, arrows and different colors denote subsequent flows (see text). The elements below the main diagonal are all zero. <https://doi.org/10.1088/1742-5468/2015/05/P05011> ©SISSA Medialab Srl. Reproduced by permission of IOP Publishing. All rights reserved.

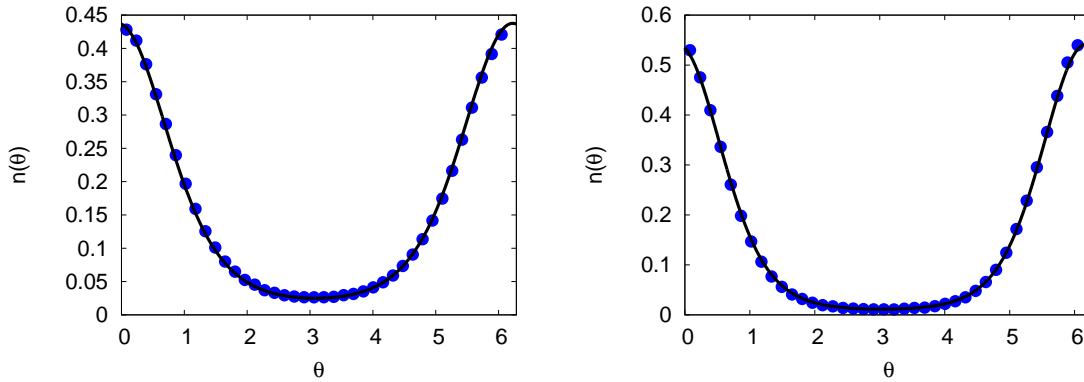


Figure 10. Density $n(\theta)$ in the dynamics (44) with a Gaussian $g(\omega)$, for $m = 0.25$, $T = 0.25$, $\sigma = 0.295$, $k_{\text{trunc}} = 12$ (left panel), and for $m = 5.0$, $T = 0.25$, $\sigma = 0.2$, $k_{\text{trunc}} = 2$ (right panel). Simulations results are denoted by points and pertain to number of oscillators $N = 10^6$, while theoretical predictions are denoted by lines. <https://doi.org/10.1088/1742-5468/2015/05/P05011> ©SISSA Medialab Srl. Reproduced by permission of IOP Publishing. All rights reserved.

of the Hermite functions implies that

$$n(\theta) = \int_{-\infty}^{\infty} d\omega g(\omega) b_0(\theta, \omega), \quad (69)$$

$$p(\theta) = T \int_{-\infty}^{\infty} d\omega g(\omega) \left(\sqrt{2} b_2(\theta, \omega) + b_0(\theta, \omega) \right). \quad (70)$$

We thus need the coefficients $b_0(\theta, \omega)$ and $b_2(\theta, \omega)$, whose evaluation requires truncating the expansion (60) at suitable values k_{trunc} of k . Figure 9 implies that knowing $c_{2,2k}$ allows to compute $c_{0,2k}$, so it is natural to choose the same k_{trunc} for both $b_0(\theta, \omega)$ and $b_2(\theta, \omega)$.

In Figs. 10 and 11, we demonstrate an excellent agreement between theory and simulations for given values of (m, T, σ) . From the figure, it is evident that our analytical approach works very well for both small and large values of m .

The ratio $p(\theta)/n(\theta)$ gives the temperature $T(\theta)$. Equilibrium state of a system necessarily implies a spatially uniform temperature profile, i.e., $T(\theta)$ equals the temperature T , independent of θ , where T is the temperature of the heat bath the system is in contact with. The spatially non-uniform temperature profile in the right panel of Fig. 11 lends further credence to the suggestion that the synchronized state we are dealing with is a NESS. The figure also shows a density-temperature

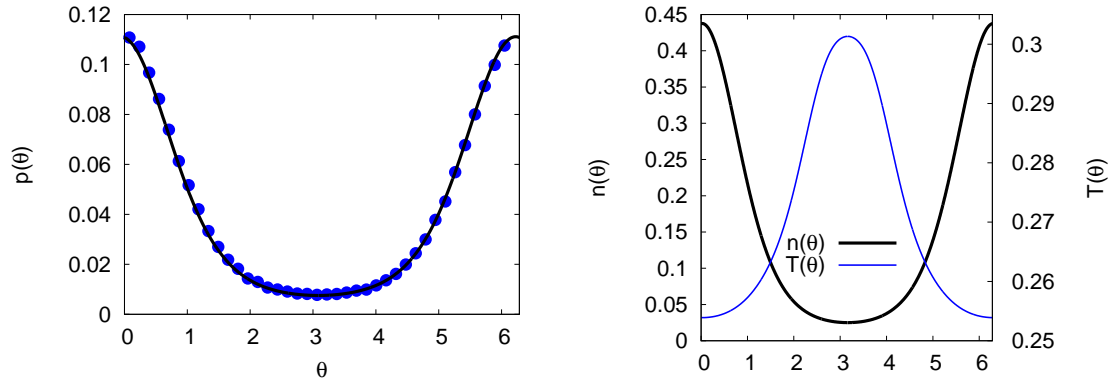


Figure 11. In the left panel is shown the pressure $p(\theta)$ for the same parameters as for the left panel of Fig. 10. Simulation results are depicted by points and pertain to number of oscillators $N = 10^6$, while theoretical predictions are denoted by lines. In the right panel is shown the local temperature $T(\theta) = p(\theta)/n(\theta)$ and its anticorrelation with the density $n(\theta)$. <https://doi.org/10.1088/1742-5468/2015/05/P05011> ©SISSA Medialab Srl. Reproduced by permission of IOP Publishing. All rights reserved.

anticorrelation, i.e., the temperature is peaked at a value of θ at which the density is minimum, and vice versa. This phenomenon of temperature inversion has been argued to be a generic feature of long-range interacting systems in NESSs [45, 46, 47].

5. Conclusions

In this review, we presented an overview of statistical mechanical aspects of large networks of coupled phase oscillators with distributed natural frequencies. We analyzed an issue of both theoretical and practical relevance, namely, the conditions under which the system displays the emergent phenomenon of spontaneous synchronization, whereby a macroscopic population of oscillators exhibits in-phase oscillations. Considering a general unimodal distribution of the natural frequencies, we discussed about phase transitions that occur between a synchronized phase and an unsynchronized/incoherent phase on tuning of dynamical parameters. While the initial part of the review focussed on the celebrated Kuramoto model involving first-order overdamped dynamics of a system of globally-coupled phase oscillators, the central part was devoted to discussing recent results obtained for a generalized Kuramoto model that includes effects of inertial terms and stochastic noise, with the underlying dynamics being second order in time. In the limit of zero noise and inertia, the dynamics reduces to that of the Kuramoto model, while at finite noise and inertia but in the absence of natural frequencies, the dynamics becomes the canonical ensemble dynamics of a paradigmatic model to study static and dynamic properties of long-range interacting systems, namely, the Hamiltonian mean-field (HMF) model. For the generalized model, we discussed how a combination of competing dynamical effects results in a rather rich and complex phase diagram in the stationary state. In particular, for a general unimodal frequency distribution, we reported the complete phase diagram of the model, and demonstrated that the system undergoes a nonequilibrium first-order phase transition from a synchronized phase at low values of the dynamical parameters to an incoherent phase at high values. In proper limits, the phase diagram incorporates the known phase transitions of the Kuramoto and the HMF model. Following the work on the generalized model reported in this review, there has been a huge surge in interest in studying the model and its extension, leading to a number of recent publications in the area. Some representative ones are Refs. [48, 49, 50, 51, 52, 53, 54, 55]. This review was entirely devoted to studies of mean-field interaction between the oscillators, namely, the case where every oscillator interacts with

every other with a strength that is the same for every pair, thereby representing an extreme case of long-range interactions. However, to model specific situations of interest, the setup has also been generalized to consider the case in which the oscillators interact with one another with a strength that decays with the spatial separation between the oscillators [56]. Recent results within such a setup and with a focus similar to the present review may be found in Refs. [57, 58].

In conclusion, we believe that a statistical mechanical approach to study a system of globally-coupled phase oscillators provides a useful tool for investigating the collective behavior of the system, and allows to deepen our understanding of peculiar features of nonequilibrium stationary states *vis-à-vis* equilibrium, besides offering new and exciting opportunities of experimental exploration.

Acknowledgements

Stefano G is grateful to Giacomo Innocenti for useful discussions on the Kuramoto model. Shamik G especially thanks Alessandro Campa for several useful and insightful discussions and comments on the Kuramoto model, and, in particular, on its derivation using the phase approximation technique as discussed in this review. We thank the Max Planck Institute for the Physics of Complex Systems, Dresden, Germany, for the hospitality during the workshop “Dynamics of Coupled Oscillators: 40 years of the Kuramoto model,” where this paper was conceptualized.

References

- [1] A. Pikovsky, M. Rosenblum and J. Kurths, *Synchronization: A Universal Concept in Nonlinear Sciences* (Cambridge University Press, Cambridge, 2001).
- [2] S. H. Strogatz, *Sync: The Emerging Science of Spontaneous Order* (Hyperion, New York, 2003).
- [3] M. Rosenblum and A. Pikovsky, *Contemporary Physics* **44**, 401, (2003).
- [4] A. Pikovsky and M. Rosenblum, *Scholarpedia* **2**, 1459 (2007).
- [5] M. Bier, B. M. Bakker and H. V. Westerhoff, *Biophys. J.* **78**, 1087 (2000).
- [6] J. Buck, *Quart. Rev. Biol.* **63**, 265 (1988).
- [7] K. Wiesenfeld, P. Colet and S. H. Strogatz, *Phys. Rev. E* **57**, 1563 (1998).
- [8] K. Hirose, S. Kittaka, Y. Oishi, F. Kannari and T. Yanagisawa, *Opt. Express* **21**, 24952 (2013).
- [9] A. T. Winfree, *The Geometry of Biological Time* (Springer, New York, 1980).
- [10] G. Filatrella, A. H. Nielsen and N. F. Pedersen, *Eur. Phys. J. B* **61**, 485 (2008).
- [11] M. Rohden, A. Sorge, M. Timme and D. Witthaut, *Phys. Rev. Lett.* **109**, 064101 (2012).
- [12] Y. Kuramoto, *International Symposium on Mathematical Problems in Theoretical Physics, Lecture Notes in Physics, Vol. 39* edited by H Araki (Springer, New York, 1975).
- [13] M. Antoni and S. Ruffo, *Phys. Rev. E* **52**, 2361 (1995).
- [14] R. Livi and P. Politi, *Nonequilibrium Statistical Physics: A Modern Perspective* (Cambridge University Press, Cambridge, 2017).
- [15] S. H. Strogatz, *Nonlinear Dynamics And Chaos: With Applications To Physics, Biology, Chemistry, And Engineering* (Westview Press, Boulder, 2014).
- [16] H. Nakao, *Contemporary Physics* **57**, 188 (2015).
- [17] Y. Kuramoto, *Chemical oscillations, Waves and Turbulence* (Springer, Berlin, 1984).
- [18] S. H. Strogatz, *Physica D* **143**, 1 (2000).
- [19] J. A. Acebrón, L. L. Bonilla, C. J. P. Vicente, F. Ritort and R. Spigler, *Rev Mod Phys* **77**, 137 (2005).
- [20] S. Gupta, A. Campa and S. Ruffo, *J. Stat. Mech. Theory Exp.* R08001 (2014).

- [21] S. Gupta, J. Phys. A: Math. Theor. **50**, 424001 (2017).
- [22] S. Petkoski and A. Stefanovska, Phys. Rev. E **86**, 046212 (2012).
- [23] B. Pietras and A. Daffertshofer, Chaos **26**, 103101 (2016).
- [24] L. Basnarkov and V. Urumov, Phys. Rev. E **78**, 011113 (2008).
- [25] K. Huang, *Statistical Mechanics* (Wiley, New York, 1987).
- [26] H. Sakaguchi, Prog. Theor. Phys. **79**, 39 (1988).
- [27] C. W. Gardiner, *Handbook of Stochastic Methods for Physics, Chemistry and the Natural Sciences* (Springer, Berlin, 1983).
- [28] H. Risken, *The Fokker-Planck Equation: Methods of Solution and Applications* (Springer, Berlin, 1996).
- [29] H. Tanaka, A. J. Lichtenberg and S. Oishi, Phys. Rev. Lett. **78**, 2104 (1997).
- [30] J. A. Acebrón and R. Spigler, Phys. Rev. Lett. **81**, 2229 (1998).
- [31] H. Hong, M. Y. Choi, B-G. Yoonk, K. Park and K-S. Soh, J. Phys. A: Math. Gen. **32**, L9 (1999).
- [32] J. A. Acebrón, L. L. Bonilla and R. Spigler, Phys. Rev. E **62**, 3437 (2000).
- [33] S. Gupta, A. Campa and S. Ruffo, Phys. Rev. E **89**, 022123 (2014).
- [34] S. Inagaki, Prog. Theor. Phys. **90**, 577 (1993).
- [35] A. Campa, T. Dauxois and S. Ruffo, Phys. Rep. **480**, 57 (2009).
- [36] F. Bouchet, S. Gupta and D. Mukamel, Physica A **389**, 4389 (2010).
- [37] A. Campa, T. Dauxois, D. Fanelli and S. Ruffo, *Physics of Long-Range Interacting Systems* (Oxford University Press, Oxford, 2014).
- [38] Y. Levin, R. Pakter, F. B. Rizzato, T. N. Teles and F. P. C. Benetti, Phys. Rep. **535**, 1 (2014).
- [39] S. Gupta and S. Ruffo, Int. J. Mod. Phys. A **32**, 1741018 (2017).
- [40] P. H. Chavanis, Eur. Phys. J. B **87**, 120 (2014).
- [41] K. Huang, *Introduction to Statistical Physics* (Taylor and Francis, New York, 2009).
- [42] N. Goldenfeld, *Lectures on Phase Transitions and the Renormalization Group* (Addison-Wesley, Reading, 1992).
- [43] A. Campa, S. Gupta and S. Ruffo, J. Stat. Mech.: Theory Exp. P05011 (2015).
- [44] G. H. Hardy, *Divergent Series* (Chelsea, New York, 1991).
- [45] L. Casetti and S. Gupta, Eur. Phys. J. B **87**, 91 (2014).
- [46] T. N. Teles, S. Gupta, P. Di Cintio and Lapo Casetti, Phys. Rev. E **92**, 020101(R) (2015).
- [47] S. Gupta and L. Casetti, New J. Phys. **18**, 103051 (2016).
- [48] M. Komarov, S. Gupta and A. Pikovsky, EPL **106**, 40003 (2014).
- [49] S. Olmi, A. Navas, S. Boccaletti and A. Torcini, Phys. Rev. E **90**, 042905 (2014).
- [50] S. Olmi, E. A. Martens, S. Thutupalli and A. Torcini, Phys. Rev. E **92**, 030901(R) (2015).
- [51] S. Olmi, Chaos **25**, 123125 (2015).
- [52] D. J. Jörg, Chaos **25**, 053106 (2015).
- [53] J. Barré and D. Métivier, Phys. Rev. Lett. **117**, 214102 (2016).
- [54] H. Chen, C. Shen, H. Zhang, G. Li, Z. Hou and J. Kurths, Phys. Rev. E **95**, 042304 (2017).
- [55] D. Yuan, F. Lin, L. Wang, D. Liu, J. Yang and Y. Xiao, Sci. Rep. **7**, 42178 (2017).
- [56] J. L. Rogers and L. T. Wille, Phys. Rev. E **54**, R2193 (1996).
- [57] S. Gupta, M. Potters and S. Ruffo, Phys. Rev. E **85**, 066201 (2012).
- [58] S. Gupta, A. Campa and S. Ruffo, Phys. Rev. E **86**, 061130 (2012).